ESRF NEWSLETTER

JANUARY 1997 EUROPEAN SYNCHROTRON RADIATION FACILITY N° 27

Diffracted intensity from the surface of a silver crystal partially covered with islands of silver atoms of monoatomic height. The central sharp peak arises from the substrate and the broad, volcano shape comes from the islands.

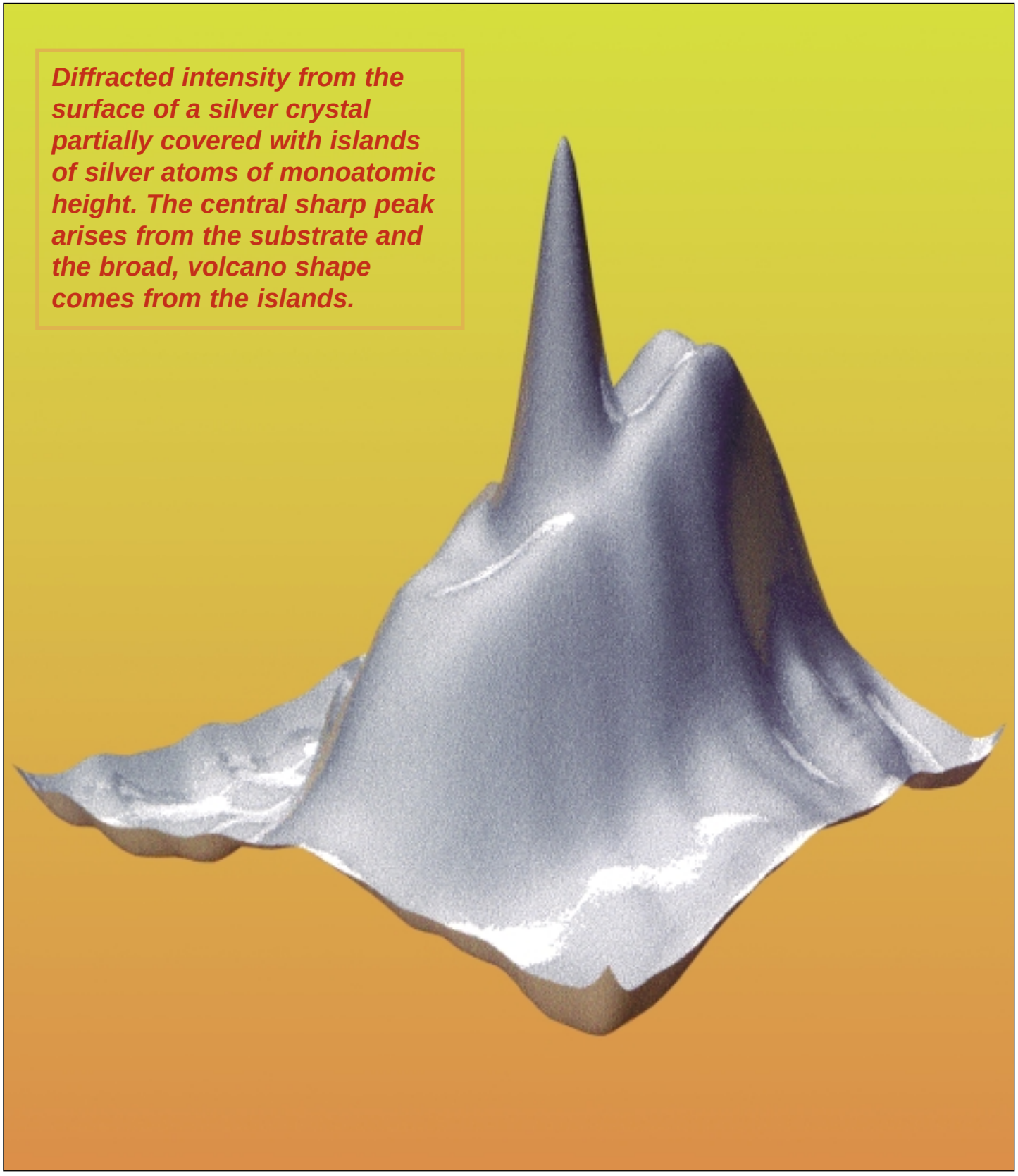

ISSN 1011-9310

CONTENTS

Photography by:
C. Jarnias, D. Marshall, H. Müllender.

HIGHLIGHT

1996 Young Scientist Award

The Users' Organisation invited nominees for the «1996 Young Scientist Award», according to the following selection criteria: «The award recognises outstanding work done in the past year at the ESRF by a scientist 40 years of age or younger.»
The winner of the award, chosen amongst eight nominees, was invited to deliver a public lecture at «Science at the ESRF» (Users' Meeting), in November 1996 and received a cash award of 5 000 FF.

Paul Loubeyre during his plenary lecture.

The announcement of the winner of the award was made during the plenary session at «Science at the ESRF» and caused last-minute readjustments of the programme, as the winner turned out to be... the plenary lecture speaker Paul Loubeyre (from Université Paris VI) «for the extension of single crystal X-ray diffraction above the Mbar, enabling the determination of the equation of state of hydrogen, of most fundamental interest and of great astrophysical relevance». Unique in its kind worldwide, the new experimental apparatus developed by P. Loubeyre has so far revealed the structural properties of various systems, among which H_2, D_2, He, LiH, H_2O, $Ar(H_2)_2$ and $Ar(O_2)_3$.

25TH MEETING OF THE ESRF COUNCIL

The 25th meeting of the ESRF Council was held in Grenoble on 27 and 28 November 1996.

BUDGET FOR 1996

The most eagerly awaited decision was that concerning the budget for 1997. After the last Council of June 1996, when a planning figure for Members' contributions of 400 MFF had been adopted, with an additional option of 408,5 MFF (cf. ESRF Newsletter N° 26), two delegations had notified the Management that they would not be in a position to support their share to a budget at this level. As a result from a Heads of Delegation meeting held on 2 October 1996, Management had had to prepare two scenarios, one providing for Members' contribution of 390 MFF and one for 380 MFF.

In the end, all delegations but the German one voted in favour of the higher level of contributions. The shortfall in contributions compared with the planning figure of June will be compensated by 10 MFF from a recent out-of-court settlement with construction contractors concerning the initial deficiencies of the experimental hall floor. This means that, together with other income of 6.8 MFF, an expenditure budget of 406.8 MFF can be funded.

MEDIUM-TERM PROGRAMME

Considering the medium-term development of the facility the Council

• endorsed the elements of a Medium-Term Scientific Programme presented by the Management and

• noted the strategic implications of reducing future budgets below the indicated level (namely that in such circumstances Management would recommend closing beamlines rather than compromising on the excellence of the facility).

The Council

• accepted that the Medium-Term Financial Estimates prepared by Management represent a reasonable basis for keeping the ESRF at the forefront and should be used to plan the future scientific programme of the ESRF but also

• recognised the difficulty faced by some Contracting Parties in meeting the implied contributions.

Therefore the Council asked the ESRF Management

• to seek Scientific Associates who will contribute to the budget of the ESRF;

• to seek other means, including further savings, of reducing contributions from Members;

• to continue to seek the means to overcome the difficult problems of increasing staff costs caused by wage drift;

in order to enable it to present to the Council budgets for 1998 and the following years in line with the availability of funds from the Member States.

The Council also considered that re-adjustments of the contribution rates of Contracting Parties should continue to be investigated. To this end, it asked the existing Working Group to continue its discussions and submit to the Council recommendations on the various items to be clarified in this context.

ARRANGEMENTS FOR THE LONG-TERM USE OF THE ESRF

Regarding Scientific Associates, the Council adopted a model arrangement to be used as a basis for negotiations with governments or scientific agencies interested in joining the ESRF at a participation level between 1% and 4% (The minimum share for full membership in the ESRF is 4%).

COLLABORATION WITH EMBL

The Council approved the «Agreement between the EMBL and the ESRF to establish a joint structural biology group (JSBG)», the principles of which had already been agreed at the last meeting.

DIRECTORS, COMMITTEES

The Council decided on the appointment of a Research Director (succession of C.I. Brändén from 1 April 1997) and of a Machine Director (succession of J.L. Laclare). The Council appointed a new Science Advisory Committee (see extra box).

SCIENCE ADVISORY COMMITTEE 1997 / 1998

F. Adams, University of Antwerpen, Belgium; **N. Allinson**, University of Manchester, United Kingdom; **M. Bolognesi**, Università di Pavia, Italy; **G. Calas**, Université de Paris VI, France; **W. Eberhardt**, Forschungszentrum Jülich GmbH, Germany; **J. Evans**, University of Southampton, United Kingdom; **R. Fourme**, LURE, France; **H. Fuess**, Technische Hochschule Darmstadt, Germany; **J. Garcia Ruiz**, Universidad de Zaragoza, Spain; **W. Hendrickson**, Columbia University, USA; **A. Jones**, Uppsala University, Sweden; **G. Krill**, LURE, France; **S. Mobilio**, Istituto Nazionale di Fisica Nucleare, Italy; **H. Möhwald**, MPI für Kolloid- und Grenzflächenforschung, Germany; **T. Paakkari**, University of Helsinki, Finland; **G. Ruocco**, Università degli Studi dell'Aquila, Italy; **G.A. Sawatzky**, University of Groningen, The Netherlands; **W. Schülke**, Universität Dortmund, Germany; **S. Sinha**, Argonne National Lab., USA; **P. Weightman**, University of Liverpool, United Kingdom; **K. Yvon**, Université de Genève, Switzerland; **T. Zemb**, CEA Saclay, France.

NEW MACHINE DIRECTOR

On 1 January 1997, Jean-Marc Filhol started his 5 year term as Machine Director.

J.-M. Filhol joined the ESRF in 1987, first as the engineer responsible for the final design, construction and commissioning of the booster synchrotron, and from 1993 as Operation Manager of the Machine Division. In April 1996, he was appointed Deputy to the Machine Director and, after the departure of J.-L. Laclare, in August 1996, became acting Machine Director.

XAFS-IX 26-30 August 1996

550 scientists meet in Grenoble to discuss X-ray Absorption Spectroscopy

At a poster session.

One hundred years after the historical report by W. K. Röntgen of the discovery of X-rays and of their differential absorption by various elements in matter, the international scientific community is still getting excited by continuously expanding applications of X-ray Absorption Spectroscopy.

Over the past decades, access to synchrotron radiation sources was a kind of revolution that has completely revivified the interest in X-ray spectroscopy and resulted in the emergence of a rich family of experimental methods grouped under the acronym «XAFS» used for X-ray Absorption Fine Structure. Typically, it was found possible to probe what sort of short range order may exist around an X-ray absorbing atom: for instance, extremely accurate interatomic distances can be derived from EXAFS spectra which combine, in a unique experiment, the local selectivity of an atomic spectroscopy with the structural sensitivity of an electron diffraction technique. It was also progressively realised that one could extract more and more refined information concerning the electronic and magnetic structure of this local probe… With time and 25 years' practice, the XAFS methods have considerably matured and are now widely accepted as a remarkable complement to X-ray crystallogaphy: this is reflected in the creation of a section dedicated to XAFS studies within the International Union of Crystallography…

The first international conference focusing on the development of the XAFS method was organised in 1981 in Daresbury (U.K.) as a «study week-end» with 80 participants. Fifteen years later, the 9th edition of this conference series (XAFS-IX) was organised in Grenoble in August 1996 by the ESRF and attracted about 550 registered delegates from all around the world: over 100 delegates came mainly from Japan but also other Asiatic countries, 100 came from North America, 25 from Russia… and 325 from Europe. Such rapid growth of a scientific community is not a marginal effect and calls for a deeper analysis. There are at least three main causes of this situation:

At the dinner.

High brilliance machines

Synchrotron radiation sources of third generation and, more specifically, the 6-8 GeV machines using undulators, allow extremely high spectral brilliance to be obtained. For the first time the X-ray spectroscopist has access to a very intense X-ray source with a tunable spectral range and full control of the polarisation of the emitted radiation, stimulating highly technical development projects all around the world. As summarised by E. Stern in his concluding remarks, in 1981 we had no optics, just slits, whereas in 1996 we can now benefit from marvellous focusing optics. There is clearly a new challenge for Europe here and it is obviously not fortuitous that the next conferences will be organised in 1998 by the American APS (Advanced Photon Source) and in 2001 by the Japanese SPring-8, facilities which are just starting or about to start operation.

Plenty of applications

The explosion of applications, not only in universities or research institutes, but also in industry, is very promising. In 1981, synchrotron radiation sources were regarded by industrial management as, at best, a matter of curiosity. In 1996, 25% of the applications of XAFS studies have an applied research finality and several European chemical companies no longer hesitate to put the various synchrotron radiation light sources into competition by developing research programmes in parallel in the U.S. and in Japan as well as in Europe. The fields where the demand for applications are most rapidly growing are included in the following list which cannot be exhaustive given the huge diversity of the problems that are addressed:

- Environmental sciences and nuclear waste contamination: the goal is to determine the chemical state of the poisoning contaminants.
- Industrial catalysis: trace amounts of highly specific elements accumulated over time are enough to poison hydrotreatment catalysts in oil industry. XAFS studies are of considerable interest to clarify the chemical mechanisms by which the active centres can be activated or deactivated.
- Chemical processes: there is indeed a

wide variety of problems and it is perhaps more convincing to concentrate on one single example. There is a joint strategic programme in the U.S. and in Europe to understand the mechanisms of oxidation of bitumens and asphalts which lead to the degradation of the highway network with time: XAFS studies are becoming increasingly used to improve the corresponding industrial process. Similar approaches also concern the control of vulcanisation processes used in the rubber and pneumatic industry.

• Biochemistry: whereas X-ray crystallography is now used to determine the 3D structure of huge macromolecules with thousands of atoms, the strategy used in XAFS studies is to concentrate only on the active centre in metalloproteins so as to detect small structural changes under the conditions of real catalytic activity. For instance, considerable progress has been made thanks to XAFS studies in the understanding of photosynthesis and of the nitrogen cycle in plants. Membrane bound proteins can even be investigated by this technique which does not require crystallisation.

• Materials science: amongst a wide variety of applications, we would like to stress here the importance of a new technique which emerged only in 1989 when the X-ray Magnetic Circular Dichroism (XMCD) was measured for the first time by G. Schütz in Hamburg. As nicely illustrated by J. Stoehr from IBM, this technique which was recently extended into the «soft X-ray range» is now of considerable importance for the optimisation of artificial magnetic thin film structures called «spin-valves». In 1988, European scientists from Thomson-CSF and CNRS discovered that such systems can exhibit a giant magnetoresistance and open up a new concept for the design of the memories of tomorrow's computers.

Progress in theory

All these interesting and sometimes spectacular applications would have been impossible without the continuous refinement of theories which contributed to transform XAFS and XMCD studies into reliable sources of quantitative information. The best example is certainly the derivation by ESRF scientists (and others) of the so-called «sum rules» for XMCD which made it possible to disentangle the respective contributions of the magnetic spin moments, the magnetic orbital moments and the magnetic anisotropy.

Science Ambassadors

How can we arouse the interest of secondary school pupils in the exciting new ways of making science in international research centres?

A new kind of answer was proposed by the ESRF with the «Science Ambassadors» project, as part of the European Week for Scientific and Technological Culture.

This project involved collaboration with CERN (European Laboratory for Particle Physics), ESA (European Space Agency), EMBL (European Molecular Biology Laboratory) and FUSION and JET (Research and Development programmes of the European Union).

Post-doctoral fellows sent to schools

On 25 and 26 November 1996, 19 post-doctoral and thesis students from EMBL, CERN, ESA, ESRF, FUSION and JET went to school, in 16 European countries. Their objective was to meet pupils and students in the school or university where they had studied themselves. They made contact with approximately 5000 youngsters in total, talked about their experience in European research centres, showed the possibilities offered to young scientists in fields such as astronomy, particle physics, biology, chemistry, space, geophysics, medicine... The pupils very much enjoyed the personal contact with a young scientist - so did the teachers, apparently, as most of them are keen to receive former students more regularly in the future.

Just after the event, the Science Ambassadors met in Grenoble on 27 November to talk about their experience, at a workshop entitled: «What can be done to improve the links between the European research centres and the educational system so that pupils can fully benefit from the very high profile of these centres?» They were convinced that direct contact with scientists was one of the best means of bringing «live» science into schools.

Brochures and posters

For this event, the ESRF decided to design teaching material specifically for secondary school level.

Brochures and posters were produced in 6 languages (English, French, German, Italian, Spanish and Swedish) so as to cover as wide an audience as possible within a reasonable budget.

These brochures and posters are available from the Information Office, tel. (33) 4 76 88 20 25, fax (33) 4 76 88 24 18, e-mail: information@esrf.fr.

SCIENTISTS REQUEST A RECORD NUMBER OF SHIFTS ON ESRF BEAMLINES

Scientists from all over the world have requested a record number of 8345 shifts on beamlines at the ESRF for the first six months of 1997. In total, a new high of 581 applications arrived by the September 1996 deadline for beam time on the 23 ESRF and 4 CRG beamlines which will be scheduling user experiments during this period.

The Review Committees, whose members are external scientific experts in a range of fields, met at the ESRF on 24 and 25 October 1996 to review the applications. Following discussions, 289 proposals were finally selected and allocated a total of 3569 shifts of beam time. **Figure 1** shows the results of these allocations per Review Committee. Almost 50% of proposals were successful this review round, compared with an average of 45% over previous rounds.

The Committees commended users on the higher quality of proposals. This largely reflects the interest in challenging projects which can be undertaken given the specific qualities of the beam at the ESRF.

The beamlines which were the most frequently requested for this round were: ID16 (Inelastic Scattering); ID2 (High Brilliance, with applications in both Small-Angle X-ray Scattering and Macromolecular Crystallography); ID24 (Dispersive X-ray Absorption Spectroscopy); ID18 (Nuclear Resonance), ID12B (Dragon Spectrometer with Polarisation Selectivity) and ID13 (Microfocus).

Figure 2 shows the number of shifts allocated compared with shifts requested, per scheduling period, since the beginning of user operation. It should be noted that the second scheduling period during each year is slightly shorter than the first, so that there are fewer shifts allocated and scheduled during the second half of each year.

Potential users are reminded that the next deadline for proposals, for beam time between July and December 1997, is

1 March 1997.

During this period the available beam time for macromolecular crystallography will be significantly increased, since two experimental stations on ID14, the Protein Crystallography beamline, will begin user operation. In addition another three new beamlines will accept users: ID21 (X-ray Microscopy); ID22 (X-ray Fluorescence Microprobe) and ID26 (X-ray Absorption Spectroscopy for Ultradilute Samples).

Proposal forms, experimental report forms and further information are available at the

ESRF Web site: http://www.esrf.fr, or from the User Office.

Fig. 1: Proposals submitted and allocated beam time, per Review Committee.

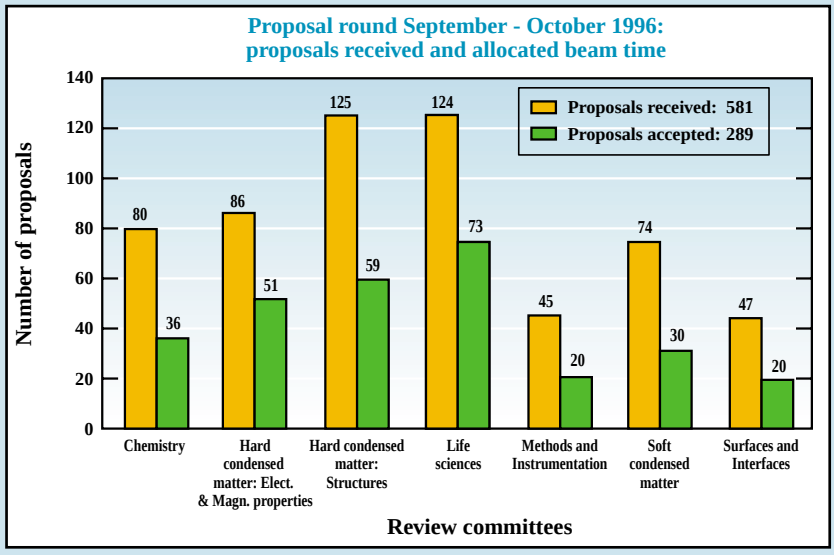

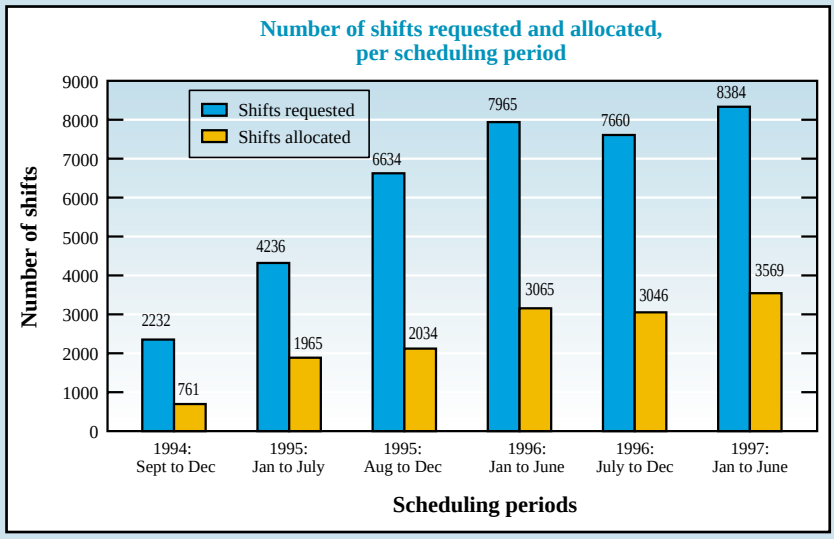

Fig. 2: Total number of shifts of beam time requested and allocated, per scheduling period.

Emplacement pub Goodfellow

«SCIENCE AT THE ESRF»

(1996 ESRF USERS' MEETING)

This year the Users' Meeting lasted three days, from Monday 18 to Wednesday 20 November. In contrast with previous years, it was decided to shift the emphasis from technical developments associated with beamline construction towards the scientific results produced at the ESRF, reflecting the fact that the ESRF and its beamlines have now reached a more mature operational state.

The meeting was opened with a plenary session at the Atria Europole Conference Centre with reports from the directors, a plenary lecture given by P. Loubeyre on «Single Crystals and Diffraction above 1 Mbar», and the announcement of the «1996 Young Scientist» who was... P. Loubeyre (see page 2)! In the afternoon, the oral programme included a selection of scientific highlights covering a wide range of scientific fields, including macro-molecular crystallography, polymer diffraction, inelastic scattering, magnetism, nuclear resonance diffraction and dynamics with coherent X-rays. The talks were mainly given by external users invited by the Users Organisation. The day ended with a poster session, covering several new technical developments of the beamlines as well as various scientific topics. A cocktail offered by the Users' Organisation was served in parallel to the poster session.

The following days were dedicated to three parallel workshops covering the fields of «X-rays and Magnetism», «Challenging Biological Structures» and «Surfaces and Interfaces» chaired by W. Eberhardt, G. Dodson and F. van der Veen respectively. Each year three different research fields will be given special emphasis. A detailed review of the workshops will soon be available.

The meeting was attended by almost 350 participants from all over the world, including Taiwan!

TRANSVERSE PROFILES OF THE X-RAY DIFFRACTED INTENSITY DISTRIBUTIONS DURING EPITAXIAL GROWTH

J. ALVAREZ, E. LUNDGREN, X. TORRELLES AND S. FERRER
ESRF, EXPERIMENTS DIVISION

Epitaxial systems grown by vapour deposition constitute one of the major areas in material research, due to their applicability to electronic devices, magnetic coatings or X-ray optical elements. The structural quality of the interfaces is a key point in determining the characteristics of a heteropitaxial system.

Many techniques have been devoted to monitor the growth process while it is occurring.

By far the most utilised one is RHEED (Reflection High Energy Electron Diffraction) since strong oscillations in the intensities of reflected beam were observed during epitaxial growth of GaAs [1,2]. The period of the oscillations corresponded to the time required to grow one atomic layer. Other techniques such as neutral atom diffraction [3] and LEED (Low Energy Electron Diffraction) [4] produced similar results and were used during the 80's to characterise the morphology of the growing films. A difficulty of the electron-based techniques (particularly RHEED) is that the diffracted intensities are affected by dynamic effects, which makes a quantitative description of morphological details of the surface based on kinematic diffraction models very difficult. This difficulty does not exist with X-ray diffraction since the interaction of the beam with the sample is much weaker. In fact, oscillations on the scattered intensities were observed already in 1988 during homoepitaxial growth of germanium [5] with the use of synchrotron radiation. More recently many other groups have successfully studied in real time structural parameters of growing surfaces.

The diffracted intensity from the surface of a growing film consists, in general, of basically two components [6]: a sharp central peak plus a broad intensity distribution. The central peak arises from the long-range order on the surface and the broad tails from shorter range correlations such as the one that exists on a surface containing a distribution of islands. Practically all the published literature refers to the temporal evolution of the peak intensity of the sharp component, although in some cases the diffuse component may contain the most significant information.

The relevant rates of growth in Molecular Beam Epitaxy studies are around one atomic layer every minute or less and this is usually too fast to record the full diffracted intensity (central peak

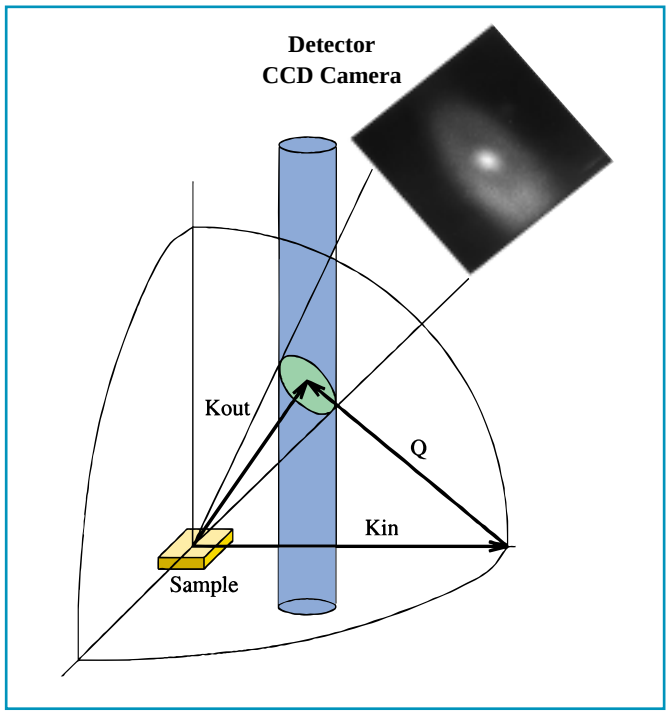

Fig. 1:
Ewald construction illustrating the scattering geometry of the intensity distribution as displayed in the front cover of this Newsletter. The surface is illuminated with the monochromatic X-ray beam of wavector K_{in} at grazing angles. In the direction of the outgoing wavector (K_{out}), a CCD camera is installed. The elliptical contour of the image arises from the cut of the diffraction rod by the Ewald sphere as depicted in the figure as a shaded area. The central white spot in the image is the intensity resulting from the long range correlations. Its three-dimensional representation in the frond cover (also Figure 2) shows a sharp, well-defined peak. Around the central peak, the diffuse scattering is apparent, looking like a volcano.

plus diffuse tails) without interrupting the growth. However, the advent of high-brilliance synchrotron beams such as the ones at the ESRF, combined with the performances of the CCD detectors, offers new possibilities to these studies as will be shown below.

We will first illustrate with an example how the central peak and diffuse tails may be shown with a CCD camera.

One has to bear in mind that, due to the two-dimensional nature of a surface, the reciprocal space consists in an ordered array of rods perpendicular to the surface plane. The rods are sharp in the directions parallel to the surface and they are extended along the surface normal direction. Due to this, the Ewald construction to determine the diffraction conditions, differs slightly from that of a three-dimensional sample. **Figure 1** shows the Ewald construction appropriate to the surface scattering experiments. The incoming wavevector is grazing the sample surface and the outgoing one makes an angle with the surface which depends on the scattering vector Q. The intersection of one of the rods (its diameter has been very exaggerated for clarity) with the Ewald sphere results in an quasi-elliptical shape as shown in the shaded area. This ellipse determines the angular distribution of diffracted intensity. The image shown in the figure is a real image of a surface taken with a CCD camera located in the direction of K_{out}. One can clearly see the elliptical shape resulting from the intersection of the rod with the Ewald sphere and the central component as a more intense white spot in the middle. **Figure 2** (front cover page) is a three-dimensional representation of that CCD image with appropriate filtering and smoothing. There, the central peak emerges very clearly from a volcano-shaped diffuse distribution. The surface that originated such a distribution was the (100) face of an Ag crystal partially covered (50%) by two-dimensional islands (only one atom in height) of Ag atoms. For this particular coverage, the short-range correlations are enhanced, which allows us to better distinguish both components of the scattered intensity.

Analysis of the diffuse scattering allows us to determine some average values of the statistical distribution of Ag islands. The existence of two maxima in the diffuse scattering, symmetrically located around the central component, is

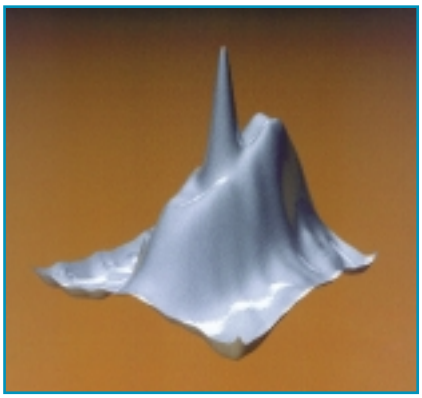

Fig. 2:
Diffracted intensity from the surface of a silver crystal partially covered with islands of silver atoms of monoatomic height. The central sharp peak arises from the substrate and the broad, volcano-shaped distribution from the islands.

an indication of a rather well-defined correlation length. The magnitude of this correlation length is simply π/(separation of the diffuse peaks) which in our example results in about 100 Angstroms. This is the characteristic length scale of the island distribution which gives the average separation between the islands.

Figure 2 was taken after interrupting the growth process, cooling the sample to freeze the atomic diffusion and exposing it to X-rays for 30 minutes. These are certainly not the ideal conditions for studying epitaxial growth. It would be more desirable to take images of the diffracted intensity while the crystal is growing. This can be achieved if one performs a one-dimensional integration by binning the CCD. This means that all the 1024 columns of the CCD can be added together to improve statistics. Under these conditions the CCD acts as a one-dimensional detector.

The non-interrupted growth experiments were done in a different scattering geometry from that depicted in Figure 1. Both the incoming and exit angles were grazing the surface. Under these conditions the eccentricity of the ellipse is very large since the major axis, directed along the rod, is much larger that the minor one. This geometry, together with the binning of the CCD allowed us to obtain cuts of the diffracted intensity distribution along a direction parallel to the surface of the sample. Some examples of these transverse intensity distributions are shown in **Figure 3**. The advantage of this experimental set-up is that every line profile in Figure 3 was taken with only two seconds of exposure to the beam. This relatively short time allows us to record the line scans while the crystal is growing, at a rate of about one atomic layer per minute, and to take "a movie" of the growth process.

The type of results that one finds are illustrated in Figure 3. All the profiles correspond to different experiments of

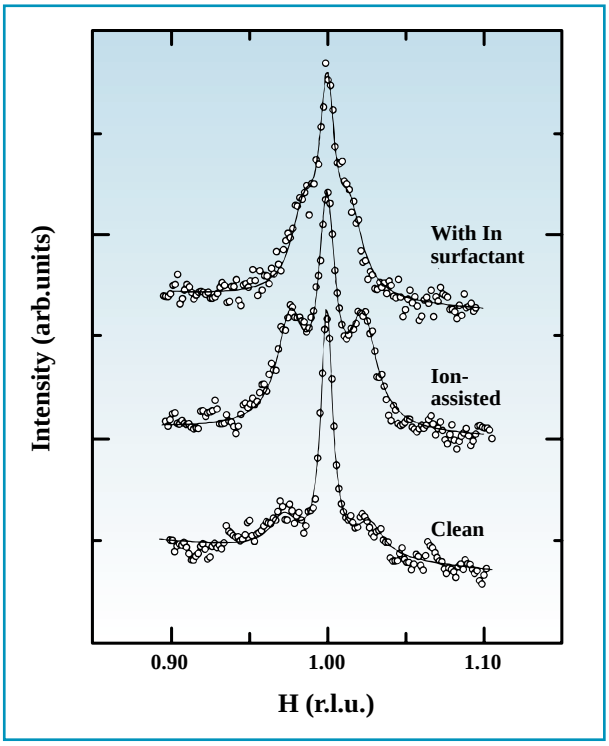

Fig. 3:
Transverse profiles of the diffracted intensity recorded during non-interrupted epitaxial growth experiments. Each profile was recorded in 2 seconds of exposure to the beam. The readout time was 1.3 second. Three different profiles have been chosen to illustrate how the diffuse scattering may be different depending on the growth conditions (see text for details).

non-interrupted growth of Ag on Ag (100), while the first atomic layer is growing and the starting substrate surface is covered approximately by 50% of islands. In all cases the deposition rate is of one atomic layer every 90 seconds and the sample temperature is 330 K.

The bottom profile ("clean") is taken from a surface growing without any external disturbance or manipulation. The diffuse component is much lower in intensity than the central peak, indicating that the long range correlations are the dominating ones at the surface.

The second profile ("ion-assisted") results from a similar experiment except that the growth was performed while the surface was bombarded at low dose with inert gas ions (Argon) at 1 keV. The diffuse scattering component is more intense than that of the previous experiment. The two symmetrical peaks around the central peak indicate a well-defined distance between the islands. The separation of the diffuse component from the central peak is 0.02 in reciprocal lattice units. This means that the average island separation is approximately 127 Angstroms. The inert gas ions probably dynamically generate nucleation centres for the islands. Similar results have been obtained recently with STM (Scanning Tunneling Microscopy) studies [7].

The top line profile ("with In surfactant") results from a growth process manipulated with a surfactant since the substrate was precovered with about 10% of an atomic layer of indium atoms before starting the Ag growth. As may be seen by comparing this profile with the previous one, the two peaks of diffuse scattering are closer to the central peak. In this case the average island distance is 209 Angstroms.

In summary, the intense beams at the ESRF and the CCD detection technique allow the study of epitaxial growth processes in a more detailed way that what has been done up to now. Under the appropriate scattering conditions, it is possible to perform experiments of non-interrupted growth, at rates of around 1 atomic layer per minute, while recording transverse profiles of the diffracted intensity containing the long range order contribution and the diffuse scattering. ■

References

[1] J.H. Neave, B.A. Joyce, P.J. Dobson and N. Norton, Appl. Phys. A31 (1983)1

[2] M. van Hove. C.S. Lent. P.R. Pukite and P.I. Cohen, J. Vac. sci, and Technol. B3 (1983) 741

[3] L. J. Gomez, S. Bourgeal, J. Ibanez and M. Salmeron Phys. Rev. B31 (1985) 2551] and J. de Miguel, A. Cebollada, JM. Gallego, J. Ferron and S. Ferrer, Jour. of Cryst. Growth 88 (1988) 442

[4] M. Horn, U. Gotter and M. Henzler NATO ASI Series Physics vol 188, pg 463, 1988

[5] E. Vlieg, A. W. Denier van der Gon, J. van der Veen, J. E. Macdonald and C. Norris, Phys. Rev. Lett. 61 (1988) 2241

[6-7] P. I. Cohen, G. S. Petrich, P. R. Pukite, G. J. Whaley and A. S. Arrot, Surf. Sci. 216, 222 (1980)

[7] S. Esch, M. Breeman, M. Morgenstern, T. Michely and G. Comsa, Surf. Sci. 365 (1996) 187.

ACKNOWLEDGEMENTS

The results presented above have required a correct operation of the CCD camera and its associated software. We are very grateful to V. Rey and J. Klora for their work on this topic. Also, we thank their assistance in critical moments (such as Saturday evening or Sunday) since otherwise several of the successful experiments presented above would not have been done.

STRUCTURAL DYNAMICS OF MOTOR PROTEINS DURING MUSCLE CONTRACTION

I. DOBBIE[1], G. PIAZZESI[2], M. RECONDITI[2], P. BÖSECKE[3], O. DIAT[3], M. IRVING[1] AND V. LOMBARDI[2]

1 DEPARTMENT OF BIOPHYSICS, CELL AND MOLECULAR BIOLOGY, KING'S COLLEGE, LONDON (UK)
2 DIPARTIMENTO DI SCIENZE FISIOLOGICHE, UNIVERSITY DEGLI STUDI DI FIRENZE, (ITALY)
3 ESRF, EXPERIMENTS DIVISION

Structural dynamics of motor proteins during muscle contraction can be investigated with adequate time resolution only with high brilliance synchrotron radiation. Time-resolved Small-Angle X-ray Scattering (SAXS) experiments combined with fast time-resolution and physiological kinetics as well as high spatial resolution data from protein crystallography are crucial for solving the problem of how the molecular motor in muscle works.

Muscle contraction results from cyclical, asynchronous interactions between the myosin heads (the cross-bridges), extending from the thick filament, and the thin actin filament. In each interaction, force and filament sliding in the shortening direction are attributed to a structural change (the working stroke) in the myosin head, occurring at a rate of about 1000 s^{-1} [1, 2].

The energy liberated in each attachment-detachment cycle is thought to be provided by the hydrolysis of one ATP molecule, but the mechanism of chemomechanical transduction and the accompanying structural change still represent one of the fundamental unsolved problems of biology.

High resolution mechanical experiments performed in single muscle fibres, where it is possible to synchronise cross-bridge action by step length perturbations controlled at the level of the functional unit (the sarcomere), have shown that the amount of interfilamentary sliding accounted for by the execution of the working stroke in the attached cross-bridges is 5-10 nm [3, 4].

The ordered spatial arrangement of the contractile proteins in the myofilaments and of the myofilaments in the sarcomere makes X-ray diffraction an ideal technique for investigating the structural changes accompanying contraction. In this approach the integrity of the sarcomeric structure is maintained and direct information on molecular events is obtained under the appropriate mechanical conditions. The main limits of this technique is that the muscle is a relatively poor diffractor and that, in single frog muscle fibres, the diffracting mass is very small (fibre diameter is typically 150 µm).

In the first experiments at the ESRF, on the ID2 beamline (SAXS experimental station), two-dimensional diffraction patterns from a single intact muscle fibre from the frog Rana temporaria were collected during the development of an isometric contraction (tetanus) and during active shortening at 1/3 the maximum shortening velocity (V_0). The fibre was electrically stimulated at 4°C and at 2.15 µm sarcomere length with pulses at 25 s^{-1} frequency for 550 ms. At the plateau of the isometric contraction (300 ms after the start of stimulation) shortening at 1/3 V_0 was imposed on the fibre. A schema of the experimental apparatus is shown in **Figure 1**.

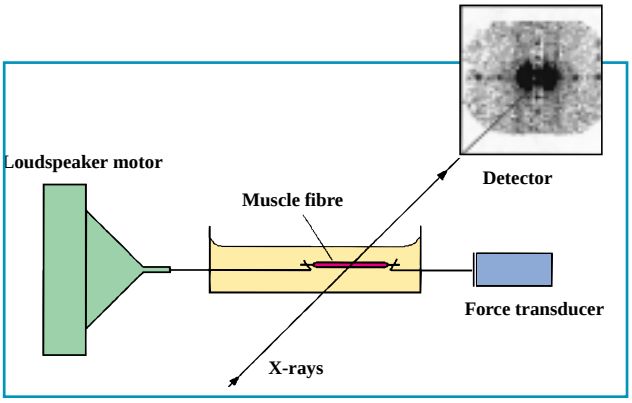

Fig. 1: Experimental arrangement for time-resolved X-ray measurements. Two-dimensional X-ray patterns were recorded with a 10-m camera length and a gas-filled detector.

In **Figure 2** the diffraction pattern from a fibre at rest (a) is compared with that at the plateau of the isometric contraction (b). Upon activation, the intensity of the (1,0) equatorial reflection reduces and the intensity of the (1,1) reflection increases, due to the mass transfer associated with the radial movement of the myosin heads from thick to thin filaments to form cross-bridges. The third order myosin meridional reflection (14.3 nm), arising from the axial mass projection of the myosin heads, remains strong but increases in width across the meridian, due to the loss of register between myofilaments. The axial spacing of the reflection increases by ~ 1.5%, probably signalling strong binding of the heads to actin. Taking advantage of the high flux and collimation of the beam at ID2, it was possible to resolve changes in the intensity and spacing of the third order myosin meridional reflection with 10 ms time resolution during rise of force

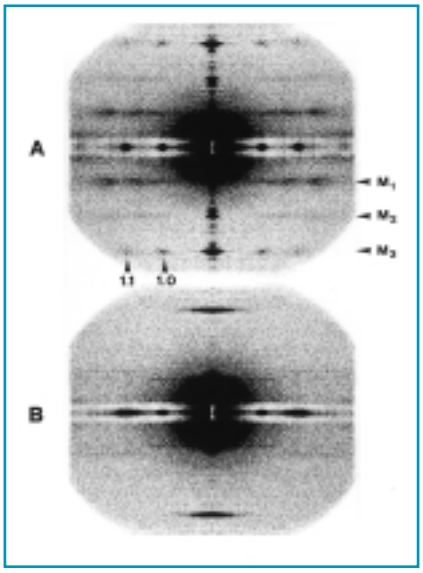

Fig. 2: Diffraction patterns from an isolated muscle fibre in the resting state (a) and at the plateau of isometric contraction (b). Each pattern is the result of a total 10 s exposure. M1 (at 42.9 nm), M2 (at 21.5 nm) and M3 (at 14.3 nm) are the first, second and third order myosin based meridional and off-meridional reflections. (1,0) (at 37 nm) and (1,1) (at 21 nm) are the most intense low-angle equatorial reflections, attenuated by an aluminium strip placed in front of the detector.

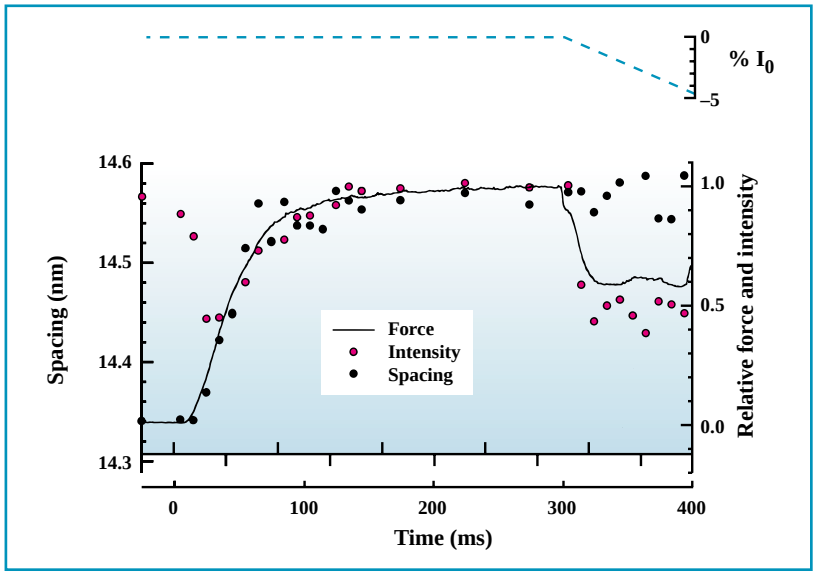

Fig. 3: Changes in the spacing and intensity of the third order myosin based meridional reflection are plotted superimposed on force during the development of an isometric contraction. Force and intensity are relative to the isometric plateau value. Zero time is the start of the train of stimulating pulses (shown in the bottom line). The X-ray data are sampled at 10 ms during the rising and shortening phases and at 50 ms elsewhere.

and during active shortening, even in a single preparation [5]. Increase in spacing of the reflection from 14.34 nm (resting value) to 14.57 nm (tetanus plateau value) follows the same time course as development of isometric force (**Figure 3**). The reflection intensity decreases abruptly, due to the loss of resting crystallographic order, then increases with a time course that almost superposes the force development and spacing change. Steady shortening at 1/3 Vo decreases the force and the intensity of the reflection to 60 and 50% of their respective isometric values, but has little effect on the axial spacing of the reflection. These results suggest that, in agreement with H.E. Huxley's original (1969) idea, myosin heads undergo a conformational change which brings the long axis of the heads more parallel to the fibre axis during the execution of the working stroke, which drives active shortening. In a simulation derived from the recent atomic model of the actin-myosin complex [6], we have tested the effect of the head movements on the intensity of 14.5 nm meridional reflection, by assuming that the light chain binding domain of the myosin head can tilt, while the catalytic domain remains rigidly attached to the actin monomer (**Figure 4**). In each picture the left part of the complex is actin with monomers in white and light cyan; the right part is the myosin head: 50 kD domain, red; 25 kD domain, green; 20 kD domain, purple; essential light chain, cyan; regulatory light chain, brown. The orientation of the light chain domain of the myosin head in A corresponds to the conformation in rigour [6] and is assumed to be that at the end of the working stroke. In B the light chain domain has been tilted by 30° about a hinge at residue 770 (indicated by the arrow), which produces a displacement of the tip of the head by ~5 nm. On the left hand side of each picture is the density of the myosin head projected onto the filament axis. Going from conformation B to conformation A the intensity of 14.5 nm reflection, obtained from the Fourier transform of the periodic density distribution, reduces to 50%. We are grateful to Ivan Rayment for providing the co-ordinates used for making this figure. ■

References

[1] H.E. Huxley, Science 164:1356-1366, 1969
[2] A.F. Huxley and R.M. Simmons, Nature 233:533-538, 1971
[3] L.E. Ford, A.F. Huxley and R.M. Simmons, J. Physiol. 269:441-515, 1977
[4] G. Piazzesi and V. Lombardi, Biophys. J. 68: 1966-1979, 1995
[5] I. Dobbie, G. Piazzesi, M. Reconditi, P. Bösecke, O. Diat, M. Irving and V. Lombardi, J. Muscle Res. Cell Motility 17:163, 1996
[6] I. Rayment, H.M. Holden, M. Wittaker, C.B. Yohn, M. Lorenz, K.C. Holmes, and R.A. Milligan, Science 261:58-65, 1993

Fig. 4: Structure of the actin-myosin complex.

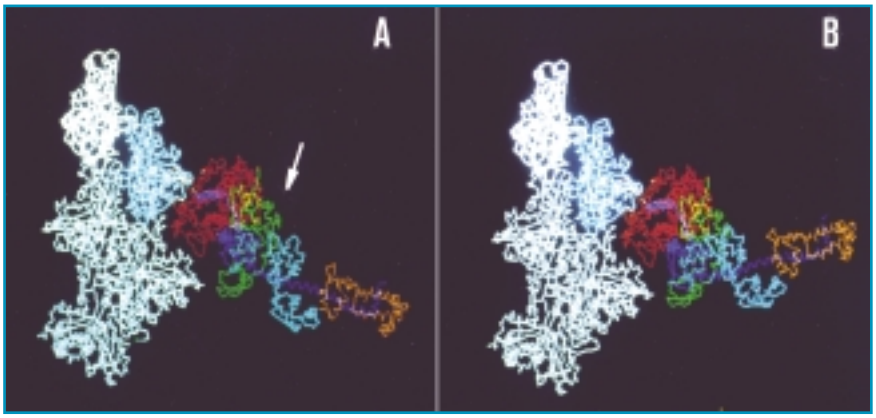

ORDERING OF CO-POLYMER THIN FILMS

G. VIGNAUD[1], A. GIBAUD[2] AND G. GRÜBEL[1]

1 ESRF, EXPERIMENTS DIVISION

2 UNIVERSITE DU MAINE, LE MANS (FRANCE)

Symmetric diblock copolymers form upon annealing a stratified lamellar structure with the lamellae oriented parallel to the surface of the substrate. This is a consequence of the incompatible character of the two species A and B which compose the structure of the diblock.

This type of ordering mandates that the film thickness in the ordered state is given by m · L where m is an integer and L is the period of the lamellar structure. For films with initial thicknesses which do not satisfy this constraint, islands or holes with a step height L are formed on the surface (**Figure 1a**).

We have studied the specular and off-specular (diffuse) X-ray scattering of ordered polystyrene (PS) / polybuthymethacrylate (PBMA) copolymer films spin-coated on Si substrates and annealed at 150 °C for 24 hours. With an initial thickness d = 430 Å, the surface of the diblock copolymer is covered with islands in the ordered state.

It appears that the periodicity in the ordered state in the direction normal to the surface in a specular scan differs from the periodicity in the same direction observed in an off-specular scan. This result is explained by an analytical calculation of the differential cross-section [1]. We characterise the diblock surface morphology, in the ordered state (**Figure 1b**), by two functions: one accounting for the shape of the islands b(r) and the other p(r) for the position distribution of the islands. We consider that the islands are cylindrical in shape with a size distribution of radii described by a log-normal distribution and they are distributed around average distances with a certain degree of disorder. A distribution developed by Hosemann for "paracrystalline" and liquid systems in which the relevant parameters are the nearest neighbour distance $\bar{d}$ and the r.m.s. (root mean square) deviation σ_n of the distribution has shown to be adequate to describe the position distribution of the islands. The transverse scans (in Q_x direction) can be well interpreted in terms of the Fourier transform of a two-dimensional function which is the convolution of the shape factor b(r) with the distribution p(r) of the islands. Observed and calculated intensities in a transverse scan parallel to the surface of the sample are shown in **Figure 1c**. One can see the very good agreement between the calculated and the measured intensity. The lineshape is well described by a radius R = 1.5 µm, an average distance $\bar{d}$ = 4.8 µm and an r.m.s deviation σ = 1.3 µm of the distribution.

Reference

[1] G. Vignaud, A. Gibaud, J. Wang, S.K. Sinha, J. Daillant, G. Grübel and Y. Gallot, J. Phys. Condens. Matter 9 (1997) LI-6.

Fig. 1:
(a) Schematic representation of the ordered surface of a symmetric diblock PS/PBMA copolymer. The film forms islands (or holes) upon annealing.
(b) Optical micrographs of a PS/PBMA copolymer film: islands appear black on a white surface.
(c) Observed and calculated intensities for a transverse scan parallel to the surface of the sample.

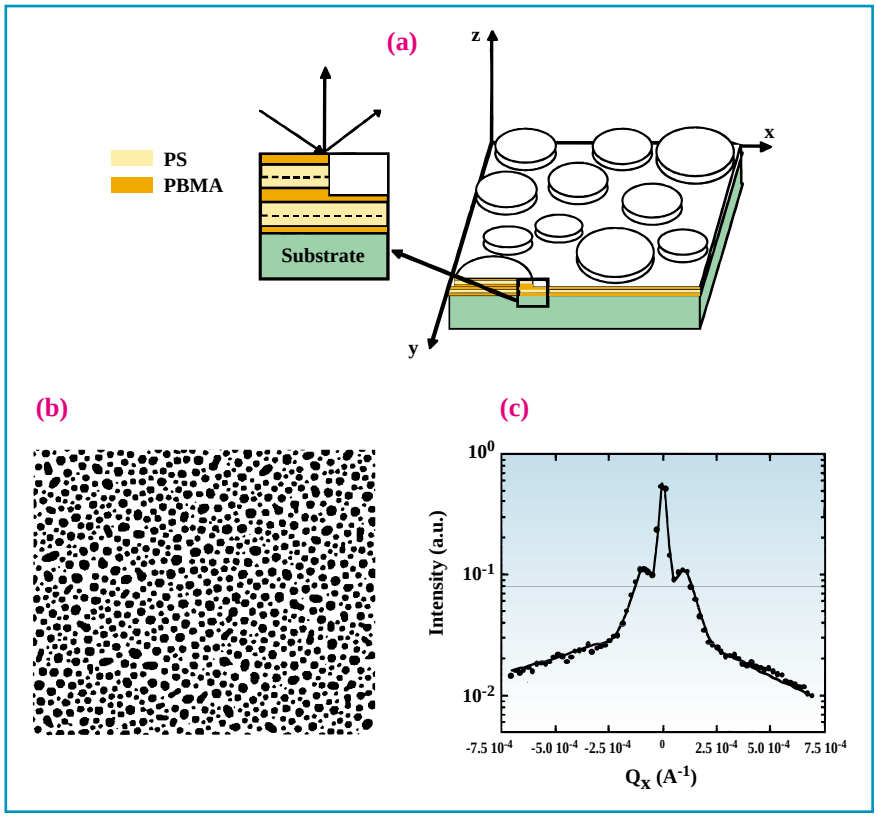

A Time Domain Picture of Transverse X-Ray Coherence

A. Q. R. Baron[1], A. I. Chumakov[1], H. F. Grünsteudel[1], H. Grünsteudel[2], L. Niesen[3] and R. Rüffer[1]

1 ESRF, Experiments Division
2 Medizinische Universität zu Lübeck, Institut für Physik (Germany)
3 Nuclear Solid State Physics, Materials Science Center, University of Groningen (Netherlands)

Transverse X-ray coherence is measured using a temporal interference pattern. This is accomplished using scattering from the very narrow 14.4 keV nuclear resonance of ^{57}Fe. Introduction of a spatial correlation in response frequencies of different nuclei modifies the measured decay, allowing information to be determined about the spatial correlations of the exciting synchrotron radiation pulse.

We present a new and different way of looking at transverse X-ray coherence. Conventionally, spatial phase correlations in field amplitudes are observed by measuring spatial interference patterns (e.g. Fraunhofer diffraction [1]). However, if the incident radiation arrives in short pulses, as is typical for synchrotron radiation, one may observe a temporal interference pattern, instead of a spatial one [2].

Consider a collection of oscillators, each having a single natural frequency but with some distribution of these frequencies from one oscillator to the next. Simple linear transform theory shows that if the response frequencies are uniformly distributed over some finite bandwidth, a well-phased excitation of those oscillators will decay with a lifetime inversely proportional to that bandwidth. Conversely, measurement of the decay time (after pulse excitation) of a collection of such oscillators allows determination of the bandwidth of those that respond in phase. If there is a correlation between an oscillators position and its emission frequency, then the measured decay time can be used to determine the spatial phase correlation of the exciting radiation.

The 14.4 keV nuclear resonance of ^{57}Fe (4.7 neV natural line width, 141 ns lifetime) acts as a single frequency oscillator. We introduce a uniform spatial gradient in the response frequency and observe the decay time of the scattering after the sample has been excited by a pulse of synchrotron radiation. By observing the speedup of the decay, we measure the spatial extent over which the exciting radiation has a well-defined phase relationship, allowing us to calculate the source size or transverse coherence length.

This work was done at the Nuclear Resonance Beamline (ID18) of the ESRF [3]. Radiation having a 6 meV bandwidth at 14.4 keV was allowed to fall onto a foil of ^{57}Fe stainless steel (SS) (see **Figure 1**). This foil was mounted on a DC motor with an axis perpendicular to the foil surface and in the horizontal plane. In this geometry, there is a vertical gradient in the velocity of the nuclei parallel to the beam direction that leads to a corresponding Doppler shift in the response frequency. The vertical displacement required to shift the resonance frequency by one natural line-width is A [μm] = 22/N [Hz], where N is the motor rotation rate. (Note that there is no gradient in the horizontal – so this geometry allows the consideration of only one dimension). Slits (15 μm high) were placed just behind the sample and just in front of the detector to limit the vertical aperture of the system. With the synchrotron run in single bunch mode (~10 mA) count rates were ~10/s in an avalanche diode detector [4].

Fig. 1: Experimental set-up. The horizontal rotation axis was inclined at 45 degrees with respect to the X-ray beam. The sample was 41 m from the source and the detector was 2.5 m downstream of the sample.

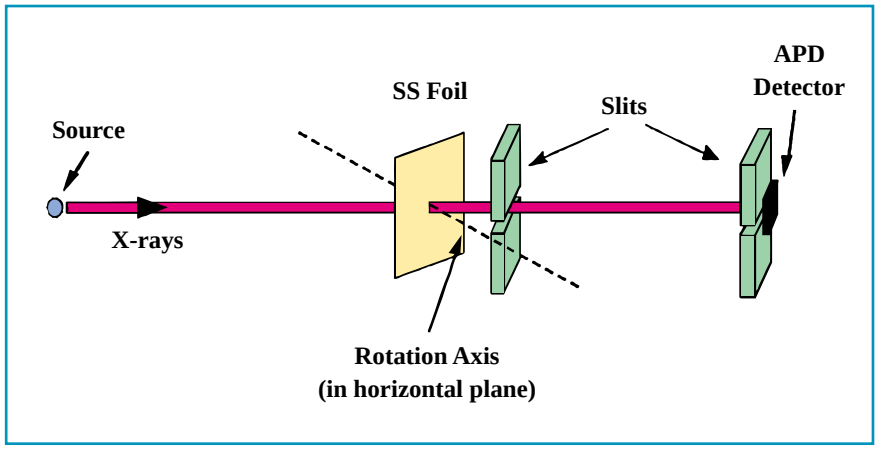

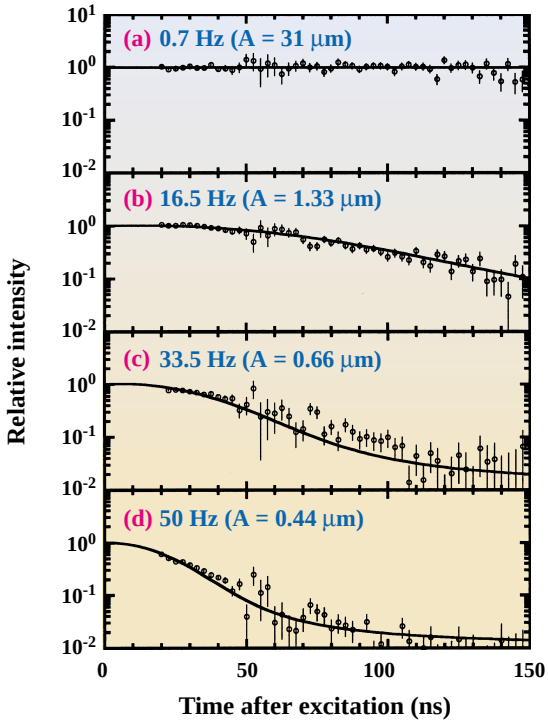

Fig. 2: Effect of rotation on the decay of the nuclear response. Faster decay at higher rotation rates indicates that there is a well defined phase relationship between scattering events from transversely separated nuclei in the foil. The vertical scale in each case is the intensity relative to the response of the foil at rest. The solid lines are fits using theory described in [2].

The measured decays are shown in **Figure 2**. The decay becomes progressively faster as the rotation rate increases, showing the expected result. The solid lines are fits using a model based on Huygens' construction (see [2]) and yield a consistent value of about 290 μm for the source size, in agreement with other measurements at ID18 [5].

Aside from allowing an alternative way of thinking about transverse coherence, this result has important implications for spectroscopic measurements using nuclear forward scattering. In particular, samples measured in such experiments are not always homogeneous in directions transverse to the X-ray beam [6]. One must then consider how to combine the scattering from transversely separated regions of the sample, coherently or incoherently. The mathematical treatment used to generate the fits above allows one to estimate that, in most cases, incoherent combination should be the rule for transverse separations greater than a few hundred angstroms. (This is due, primarily, to the large, ~mm, acceptance of the detectors used). In special cases, e.g. that described here where slits were installed before the sample and detector, this might be extended to the level of 5 to 10 microns allowing investigation of the length scale of variation in the nuclear response of the sample by observing the changes in the time response. ■

References

[1] M. Sutton, S. G. J. Mochrie, T. Greytak, S. E. Nagler, L. E. Berman, G. A. Held, and G. B. Stephenson, Nature 352, 608 (1991).

[2] A.Q.R. Baron, A. I. Chumakov, H. F. Grünsteudel, H. Grünsteudel, L. Niesen, and R. Rüffer, Phys. Rev. Lett., 77, 4808 (1996).

[3] R. Rüffer and A. I. Chumakov, Hyp. Int. 97/98, 589 (1996).

[4] A.Q.R. Baron, Nucl. Instrumen. and Meth. A 353, 665 (1994).

[5] A. Snigirev, I. Snigireva, C. Raven and M. Drakopoulos performed these measurements.

[6] H. F. Grünsteudel, H. J. Hesse, A. I. Chumakov, H. Grünsteudel, O. Leupold, J. Metge, R. Rüffer, and G. Wortmann, Hyp. Int. C 1, 509 (1996)

ACKNOWLEDGEMENTS

A. Baron would like to thank P. Cloetens for discussing this work with him. We thank the ESRF staff for making experiments possible on the Nuclear Resonance beamline, particularly J. Ejton and Z. Hubert. We thank E. Gerdau for the loan of the SS foil. H. Grünsteudel acknowledges the support of the Deutsche Forschungsgemeinschaft.

VACANCIES AT THE ESRF ON 10 JANUARY 1997

	Ref	Group	Position	Responsible
SCIENTISTS	2171/2205	Inelastic X-ray scat.	2 second beamline scientists	F. Sette
	2104	Surface science	Beamline scientist	F. Comin
	2203	Troika	Beamline scientist	G. Grübel
	PDID3	Surface science	Postdoc (ID3)	S. Ferrer
	PDID20	Magnetic scattering	Postdoc (ID20)	C. Vettier
	PDID13	Microfocus	Postdoc (ID13)	C. Riekel
	PDID16	Inelastic X-ray scat	Postdoc (ID16)	F. Sette
	PDBM29	EXAFS	Postdoc (BM29)	A. Filipponi
	PDID10A	Troika	Postdoc (ID10A)	G. Grübel
CFR	CFR200	EXAFS	Thesis student	N. Brookes

If you are interested, please send us a fax (+33 (0) 4 76 88 24 60) or an e-mail (brink@esrf.fr) with your address, and we will provide you with an application form. You can also print out an application form on the World Wide Web http://www.esrf.fr/.

On the way to Understanding the Role of Platinum in a Pt-Zeolite Catalyst

D. Sayers[1], H. Renevier[2,3], J.L. Hodeau[2,4], J.F. Berar[2], J.M. Tonnerre[2], D. Raoux[2], A. Chester[5], D. Bazin[6] and C. Bouldin[7]

1 NC STAR Project, North Carolina St. Univ., Raleigh (USA)
2 Laboratoire de Cristallographie CNRS, Grenoble
3 Univ. J. Fourier, Grenoble
4 ESRF, Experiments division
5 Mobil Technology Co., Paulsboro Techn. Center (USA)
6 LURE, Univ Paris-sud, Orsay (France)
7 NIST, Gaithersburg (USA)

The aim of this experiment was to analyse ZSM-5 zeolites, containing 3 wt.% platinum loading, by using both differential anomalous diffraction [1] and DANES (Diffraction Anomalous Near Edge Structure) methods [2]. Anomalous diffraction spectra may be able to differentiate interzeolite and intrazeolite metal particles, while DANES offers the possibility of providing chemical information about the metal inside the pores only. Our results show that such anomalous diffraction experiments can be performed on diluted powders, so that this technique may be useful for industrially important materials such as solid catalysts.

Zeolites which contain metal are an extremely important class of industrial catalysts (e.g. for reforming, cracking and dehydrogenation in the petroleum industry) [3]. In the synthesis of these catalysts, it is generally preferred that all added metal enters into the pores of the catalyst. Yet it is known that in some systems a significant amount of the metal may reside on the surface of the support particles. It is of great scientific and technological interest to measure each type of metal in order to separate their effects on the catalytic behaviour and to improve the efficiency of the synthesis so most of the metal is inside pores and, thus, more efficiently used. Spectroscopies or microscopies which are used to study these systems see all of the metal or measure an average structure and cannot differentiate between these two types of metal.

To overcome this difficulty, we have performed anomalous diffraction and DANES experiments on such zeolites at the BM2 (D2AM) beamline. The sample analysed was a Pt/ZSM-5 zeolite, containing a metal loading of about 3 wt.%

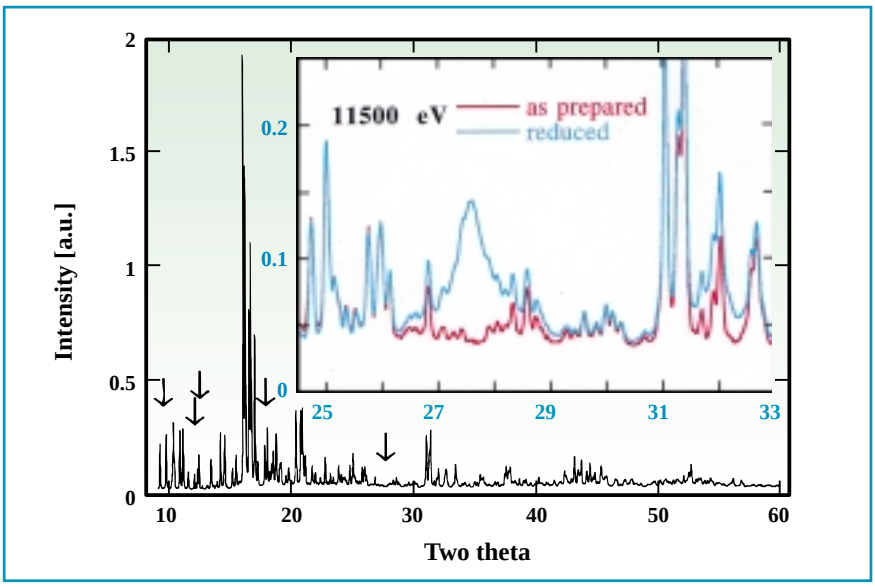

Fig. 1: Comparison of the as-prepared and the reduced zeolite ZSM-5 powder spectra close to Pt L_{III} edge (11500eV), reflections used for DANES data collection are indicated by arrows, the insert presents a spectra enlargement close to Pt (111) reflection.

Pt (somewhat higher than typical commercial systems, which contain 0.1-1% Pt). The as-prepared sample was synthesized by Mobil Co by using a common industrial procedure: ion exchange with platinum tetramine cation. The calcined sample was prepared at 350 °C in air, then reduced *in situ*, in a furnace mounted on the diffractometer, under hydrogen atmosphere.

Powder diffraction patterns were collected at wavelengths close to Pt L_{III} edge to localise platinum Pt^{2+} complex within the pores and Pt metal, in both samples. Diffraction peaks sensitive to the periodicity of the pores in the as-prepared Pt/ZMS-5 zeolite have their relative diffraction amplitudes slightly modified by the presence of the metal, indicating platinum located inside the pores. Spectra comparison of the as-prepared sample and the calcined-reduced sample show clearly fcc reflections of platinum metal (**Figure 1**). For the thermal process used, even on such a low Pt content reduced ZSM-5, a large proportion of metal particles presents the fcc structure which means that metal particles are outside pores (**Figure 2**). We must note that, on this 3wt.%Pt/ZSM-5 sample, the anomalous effect is significantly higher than the noise level. It means that differential anomalous scattering experiment could be performed at the ESRF on powders with a concentration of less than 1%.

DANES measurements have been performed on Bragg peaks of both the as-prepared and the reduced samples. The data collection was focussed on the DANES region of the spectrum to analyse the oxidation state of platinum in both samples. The (111) reflection of platinum metal and several weak reflections of the zeolite itself were chosen to separate the interzeolite information from the intrazeolite one. As strong reflections have a large contribution from the zeolite framework and provide signals relatively more sensitive to bulk absorption than to anomalous f' variation, DANES experiments were measured on weak reflection such as (231) (arrows in Figure 1). Even prior to bulk absorption correction, they show the oxidised state of platinum in the as-prepared sample, the metallic platinum in the reduced sample and the large f' variation for the Pt (111) reflection (**Figure 3**).

DAFS on powdered samples is still difficult, especially in the cases where the structure about a minority species is to be studied. These DANES measurements on a Pt/ZSM-5 sample containing 3 wt.% Pt show clear anomalous effects on weak peaks and the signal to noise is good. These results are a rigorous test of the method and demonstrate that such experiments on diluted powders can be performed at the ESRF. They provide information which is of great interest to both industrial and academic catalytic chemists in order to understand the detailed role of metals in these systems and to help synthesise improved catalysts. ■

References

[1] P.H. Fuoss et al. Phys. Rev. Lett. 46, 1537 (1981); K.S. Liang et al. J. Chem. Phys. 86, 2352 (1987); M.G. Samant et al. J. Chem. Phys. 92, 3547 (1988)

[2] H.J. Stragier et al. Phys. Rev. Lett. 69; 3064 (1992); I.J. Pickering et al. J. Am. Chem. Soc. 115, 6302 (1993); H. Renevier et al. Physica B 208&209, 215 (1995); J. Vacinova et al. J. Synchrotron Rad. 2, 236 (1995); J.L. Hodeau et al. N.I.M. B 97, 115 (1995)

[3] E. L. Wu et al. J. Phys. Chem. 83, 2777 (1979); D. G. Hay, H. Jaeger, G.W. West, J. Phys. Chem. 89, 1070 (1985); H. Van Koningsveld, H. Van Bekkum, J.C. Jansen, Acta. Cryst. B43, 127 (1987), Zeolites 10, 235 (1990); R. Goyal, A.N. Fitch, H. Jobic, J. Phys. Chem. (1996), accepted.

Fig. 2: Anomalous spectra of the reduced zeolite powder ZSM-5, at the Pt L_{III} edge 11563 eV and 11500 eV, showing fcc platinum.

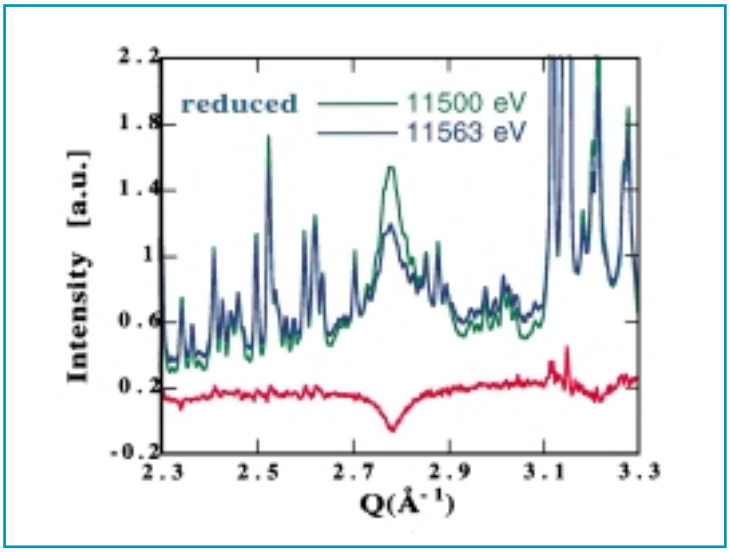

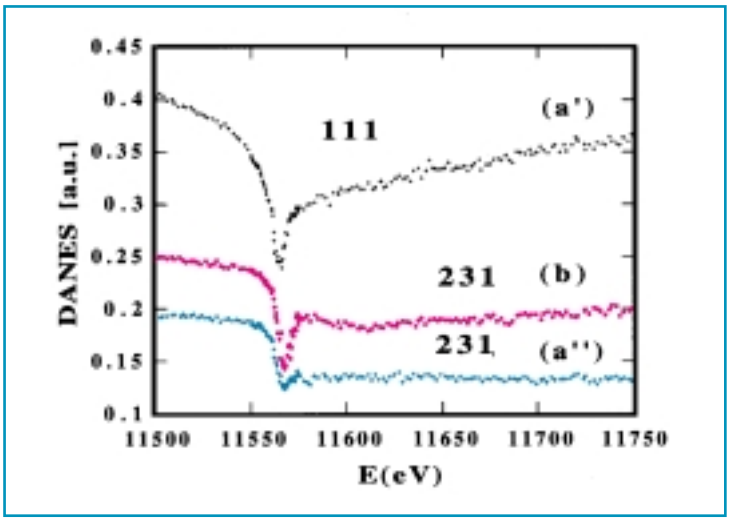

Fig. 3: DANES spectra, corrected for fluorescence of: a') (111) reflection of fcc platinum, a'') (231) reflection of the reduced ZSM-5 zeolite powder and b) (231) reflection of the as-prepared ZSM-5 zeolite powder.

Effect of the Substrate on the Orientation of Deposits of Conducting Polymers on Glass

K.E. Aasmundtveit[1], E.J. Samuelsen[1], J. Mårdalen[2] and U. Lienert[3]

1 Department of Physics, NTNU, Trondheim (Norway)
2 SINTEF Applied Physics, Trondheim (Norway)
3 ESRF, Experiments Division

Poly-octyl-thiophene (POT) is a prototype example of organic semiconducting materials, often called conjugated polymers because of the alternating single and double bonds along the polymer chain (Figure1), or conducting polymers because they become conducting when doped. The polythiophenes are considered as potential materials for applications in future all-plastic two-dimensional light-emitting diodes.

From diffraction studies on bulk samples it is known that POT is partially crystalline at room temperature. Optical absorption studies, performed on thin deposits on glass as obtained by spin casting from solutions, have shown that POT has a band gap of 2.0 eV (620 nm). POT is therefore red. POT and other polythiophenes possess the extraordinary property that the gap increases with increasing temperature, and POT turns yellow as the temperature is increased to 130 °C. For bulk samples this temperature region is known to coincide with the disappearence of crystallinity.

The present paper addresses the question as to what extent the presence of the glass substrate influences the structure and optical properties of the polymer. The deposited layers for absorption studies are too thin (of the order of 100 nm) for normal X-ray diffraction experiments. In a preliminary diffraction work on the Troika beamline using grazing incidence [1] it was found that the thin layers are indeed partially crystalline. That work failed to observe a certain reflection, the 010, a fact which was taken as an indirect indication that the polymer be oriented with its b-axis normal to the substrate surface. This point as well as temperture effects are the themes of the present investigation, using the Optics beamline BM5.

The sagittally focusing monochromator at BM5 delivers just sufficient intensity for this kind of experiment, when the polymer layers are not too thin. An experimental set-up with 0.2 mm vertical beam height and an grazing incidence angle of 0.2° suppressing scattering from the substrate was used in combination with a horizontally scanning scintillation detector. The scans revealed that, for a thick sample, both h00 (100, 200 and 300) **and** 010 were observed, whereas for a thin sample (estimated thickness ratio of five) the 010 was **not** seen, confirming the Troika results.

For convincing proof of preferred orientation, however, detection in the vertical direction is also needed. CCD-camera exposures provided the ultimate evidence (**Figure 2**): whereas for the thick layer sample the 100-reflection is distributed evenly in all directions, the thin layer is not only of a preferred orientation, but its a-axis is also confined to the substrate surface to within 1 - 2°!

The much weaker 010-reflection was not discernable from the CCD-camera exposure. But the fact it was absent in the horizontal scintillation detector scan tells us that for thin layers the **polymer strands are oriented with both their main chain (c - axis) and their octyl side chains (a - axis) flat on the substrate surface.** This finding is of great importance for understanding the optical properties of

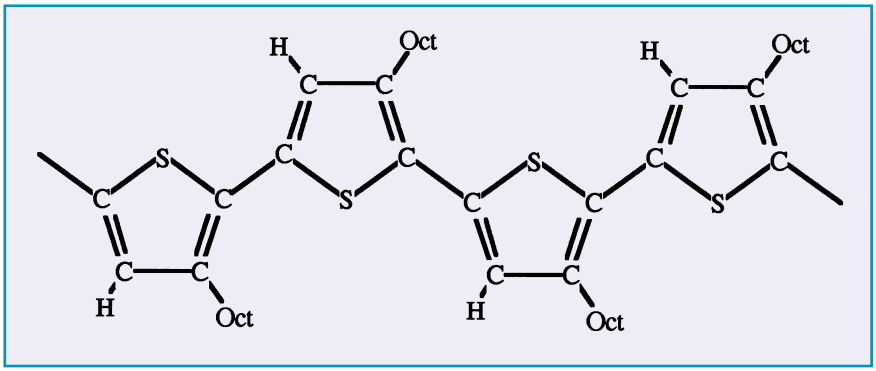

Fig. 1: Chemical structure of POT. «Oct» represents an octyl (C_8H_{17}) group.

deposited thin layers of polythiophenes. The role of various substrate materials, for instance single crystal surfaces, remains to be investigated.

Temperature studies revealed two features: the crystallinity disappears at about 130 °C, coincident with the colour change, and the preferred orientation does not reappear after heating and recooling to room temperature [2].

References

[1] H.J.Fell, E.J. Samuelsen, J.Als-Nielsen, G. Grübel and J.Mårdalen Solid State Commun. 94 843-6 (1995)

[2] K.E. Aasmundtveit, E.J.Samuelsen, J. Mårdalen and U. Lienert, to be published.

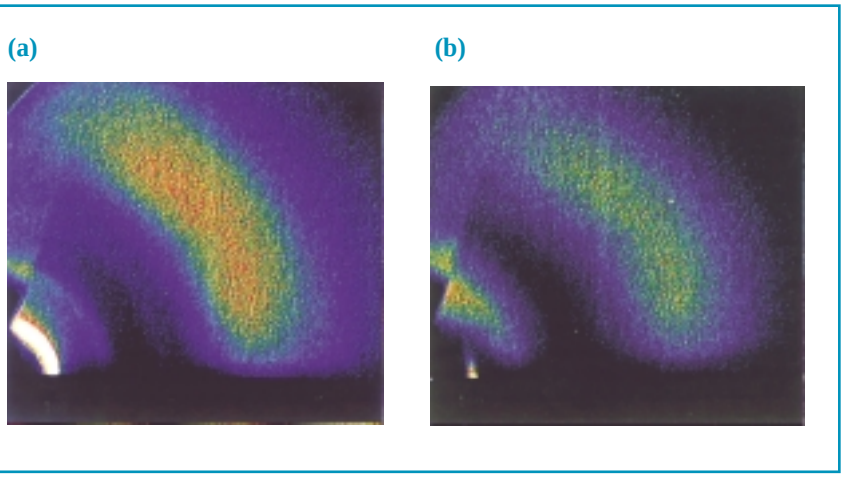

Fig. 2: CCD diffraction patterns from a) thick film and b) thin film. The direct beam is at the lower left of the image. The shadow effect on the left side is the shadow of the beam stop. a) The 100-reflection is distributed into a Debye-Scherrer ring, indicating random orientation. The broad scattering feature at higher scattering angles results mainly from the amorphous part of the polymer. The 200 and 300 reflections are also discerned. b) The 100 reflection is only seen near the horizontal direction, showing a strong orientation effect.

QUANTITATIVE TEXTURE ANALYSIS WITH A SMALL BEAM

F. HEIDELBACH AND C. RIEKEL

ESRF, EXPERIMENTS DIVISION

Quantitative analysis of crystallographic preferred orientation in polycrystals is being developed into a standard tool on the microfocus beamline (ID13). The experimental procedure is briefly described and illustrated with textures from different samples (rolled aluminum, aluminum fibres and polymer fibres).

The anisotropy of physical properties in crystals necessitates the complete analysis of the crystallographic preferred orientation (texture) in a polycrystal in order to characterise the material completely. Orientation of crystallites has a strong influence on the performance of materials as different as metals, high Tc superconductors, polymer fibres or bones. The measurement of texture with a high spatial resolution has become increasingly important with the development of microdevices with heterogeneous structures on a small scale. A complete texture analysis requires the knowledge of the orientation distribution function (ODF), which gives the volume fraction of material as a function of the orientation. The ODF can principally be deduced from two types of measurement: the analysis of complete set of diffraction data from a single crystal, or the collection of pole figures in which the orientation distribution of a single lattice plane is determined for a large number of crystals at the same time. In the first case, discrete points in the three-dimensional ODF space are measured, whereas in the second case the ODF needs to be mathematically reconstructed by inversion from the two-dimensional pole figures, e.g. [1][2]. The ODF then allows one to calculate the anisotropy of different physical parameters of the polycrystal, e.g. magnetic or elastic properties.

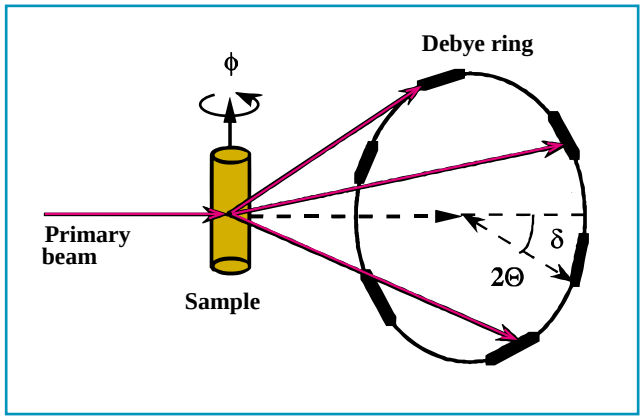

Fig. 1: Experimental set-up for texture experiments.

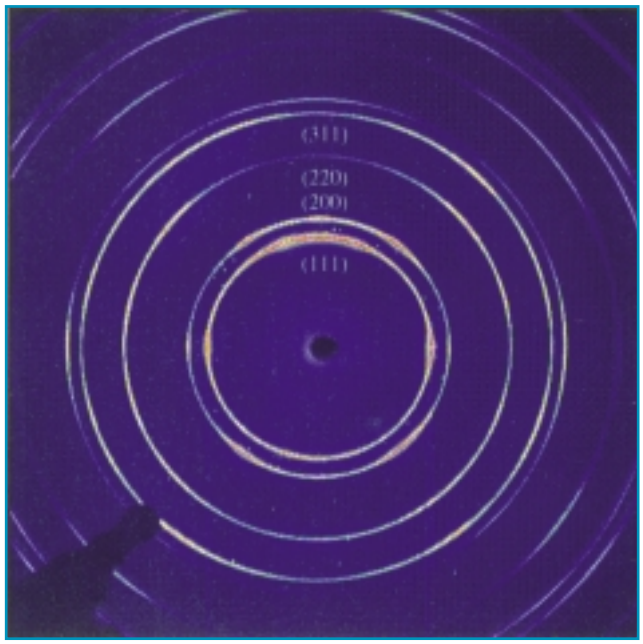

Fig. 2: Diffraction pattern from rolled aluminum at ϕ = 0.

Bäckstrøm et al. (1996) [3] performed a pilot experiment on the Microfocus beamline looking at differences in texture along the growth direction in an Fe-Ni-LIGA sample (LIGA is a micro-lithography technique). However in order to standardise the method, it appeared reasonable to go back to fairly simple samples with reasonably strong textures. Furthermore the pilot experiment was limited by the non-availability of a goniometer for sample rotation and the lack of an on-line detector. These have since been installed on the beamline.

METHOD

In the present set-up (**Figure 1**) at the Microfocus beamline (ID13) monochromatic radiation is used to generate Debye ring diffraction patterns (**Figure 2**) from small polycrystalline

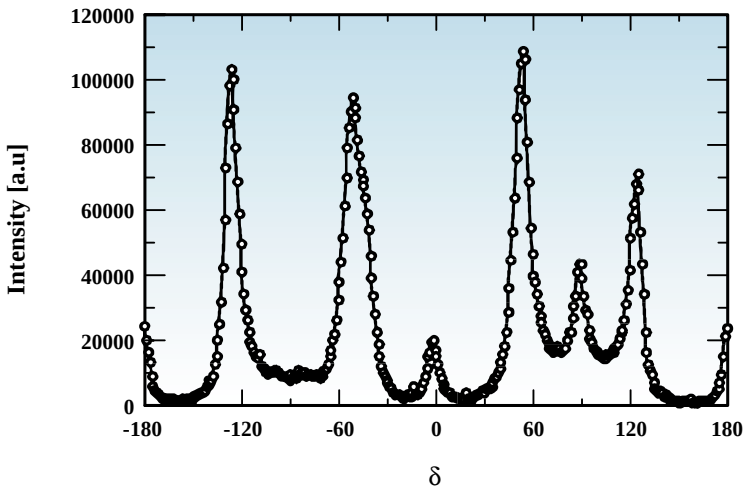

Fig. 3: Azimuthal intensity distribution of (200) ring corrected for background, polarisation and absorption.

volumes either in transmission or in reflection geometry. The intensity variation along the rings yield the orientation information for different lattice planes. The intensities are discretised, corrected for background, absorption and polarisation (**Figure 3**) and then transferred into a spherical coordinate system, i.e. into a number of pole figures (**Figure 4**). In order to fill a complete pole figure, the sample needs to be rotated around one axis. In this case we used a rotation around the vertical ϕ axis of the K geometry. The pole figures are used as input for the calculation of the true three-dimensional ODF. The calculation of the ODF is achieved with the WIMV algorithm [4] which uses an iterative approach in the determination of the ODF. The comparison between experimental and recalculated pole figures shows the consistency of the data set (**Figure 5**). The WIMV algorithm is part of the texture package BEARTEX [5] which also allows for a variety of other texture functions (manipulation of pole figures and single orientation data, calculation of physical properties etc.).

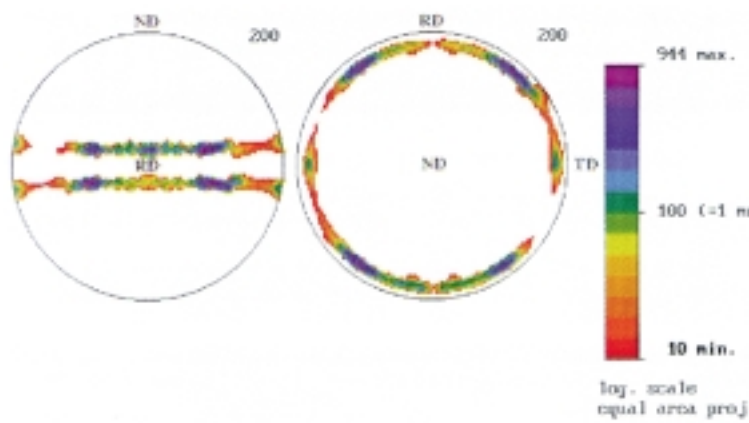

Fig. 4: Pole figure showing the position of the (200) reflections in spherical coordinates; on the left as measured, on the right rotated into standard pole figure orientation for rolled samples, compare with Figure 5a (both equal area projection); rolling (RD), transverse (TD) and normal (ND) directions are indicated.

Fig. 5: Comparison of experimental (a) and recalculated (b) pole figures of rolled aluminum; the rolling direction is N-S and transverse direction E-W; the N-S trending stripe of no data in the experimental data corresponds to the blind area inherent in the experimental set-up at high ϕ rotations; it is not used in the ODF calculation, but can be recalculated from the final ODF.

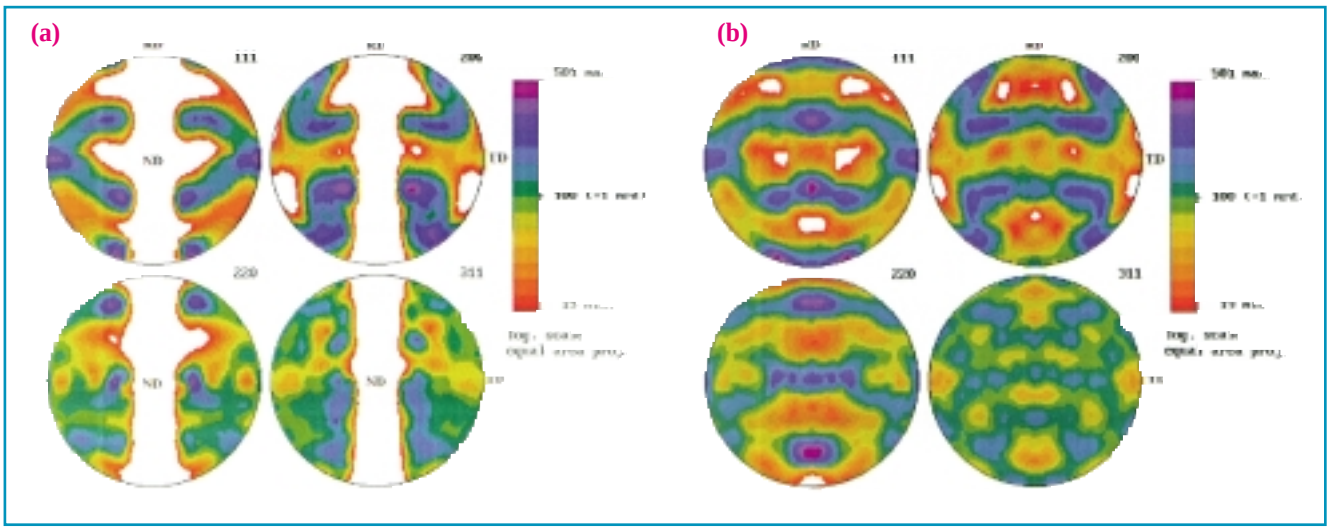

EXAMPLES

Aluminum wires

Three aluminum wires of different thicknesses (98, 150 and 200 µm) supplied by Pechiney were measured in transmission with a 30 µm beam. Diffraction patterns were recorded at 10° increments of rotation around the fibre axis covering an angular section of about 240°. All three samples show the typical (111) fibre texture with a small component of (100) (**Figure 6**). The change in thickness does not affect the type or strength of the texture, as the maxima in all three cases are similar.

Polymer fibres

Three polymer fibres (two different types of polyethylene, one Kevlar) of about 20 µm thickness were measured in transmission with a 30 µm beam. The diffraction patterns were also recorded in 10° steps around the fibre axis covering a range of about 260°. All three polymers show very strong (001) fibre textures (**Figure 7**) with the (100) and (010) planes randomly distributed around the fibre axis. However, preliminary experiments with a 2 µm beam showed domains of preferred orientation within single polyethylene fibres [6]. A more quantitative analysis of these results is in progress.

CONCLUSIONS

The quantitative analysis of crystallographic preferred orientation with high spatial resolution has been established as a standard tool on ID13. The complete textures derived from very small volumes (micron size) are principally useful in two ways:

• to analyse very small samples (i.e. thin fibres, microdevices) which have been up to now inaccessible to texture analysis;

• to detect variations and gradients of texture within samples of a larger scale which could not be resolved with previous methods of texture analysis.

The presented method fills a gap in orientation analysis that exists between more or less conventional methods of bulk texture analysis with X-rays or neutrons and the fine scale orientation analysis possible with scanning or transmission electron microscopy. ■

References

[1] H.-J. Bunge, Texture Analysis in Materials Science. Butterworths, London, (1982) 593pp.

[2] S. Matthies, G. W. Vinel & K. Helming, Standard Distributions in Texture Analysis, Akademie Verlag, Berlin, (1987) 442 pp.

[3] S. P. Bäckstrøm, C. Riekel, S. Abel, H. Lehr and H.-R. Wenk, Journal of Applied Crystallography 29 (1996) 118-124.

[4] S. Matthies, Physica Status Solidi B92 (1979) 135-138.

[5] H.-R. Wenk, S. Matthies and J. Donovan, Proceedings 11th International Conference of Textures in Materials (1996) 212-217. Int. Acad. Publ., Beijing.

[6] C. Riekel, A. Cedola, F. Heidelbach and K. Wagner Macromolecules (1996) in press.

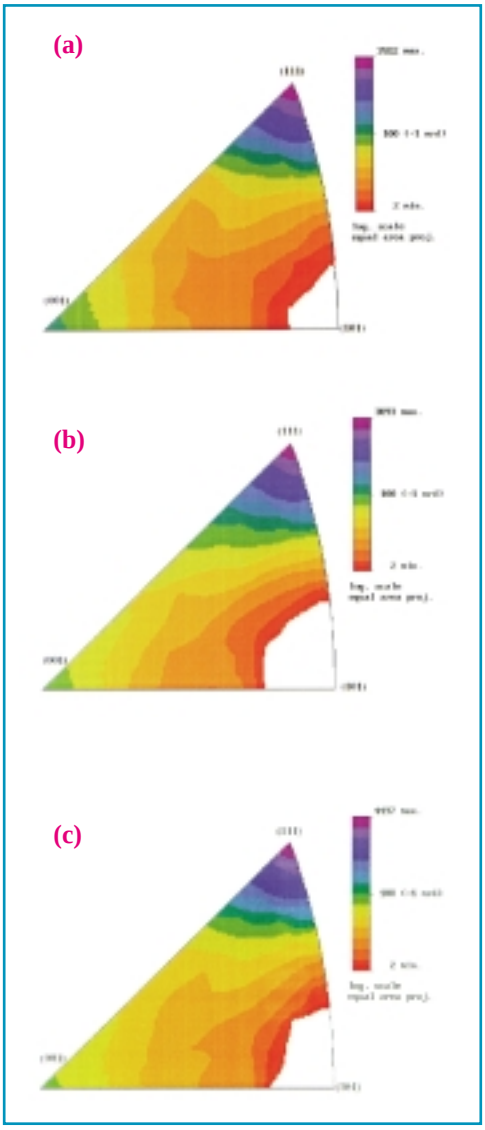

Fig. 6: Inverse pole figures (equal area projections) of the fibre axis of aluminum wires with different thicknesses; a) 98 µm; b) 150 µm; c) 200 µm.

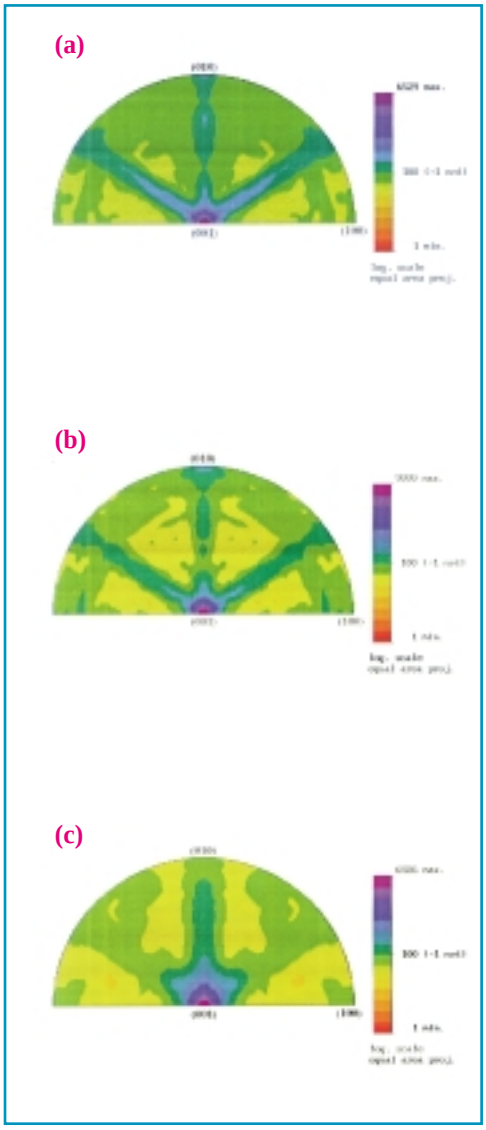

Fig. 7: Inverse pole figures (equal area projections) of fibre axes of orthorhombic polymer fibres; a,b) Polyethylene; c) Kevlar.

LATEST NEWS FROM THE MACHINE

J.M. FILHOL, MACHINE DIVISION

NEW LOW βz LATTICE FOR THE MACHINE

For some time now, extensive studies have been carried out on the evolution of characteristics of the electron and photon beams when switching from the present lattice (4 nm) to the low βz one. As clearly described in the article «The Low Emittance Lattice» published in the ESRF Newsletter No. 24 of June 1995, the gain in brilliance due to switching to the present 4 nm lattice (from the originally used 7 nm) was not maximum in the so-called «high beta straight sections». The gain in brilliance one could have expected was limited by the mismatch between the diffraction ellipse (resulting from the photon beam emittance produced by a single electron) and the electron beam ellipse (resulting from the vertical emittance and the vertical beta function βz). The benefit of any further decrease of the vertical electron beam emittance was also significantly impaired by this effect. However, by reducing the vertical beta in the high beta straight sections from 13.3 m down to 2.5 m, perfect matching is very nearly reached. Thus the photon beam vertical emittance is reduced by nearly a factor two and the brilliance is almost doubled.

The low βz lattice presents other advantages when compared with the previous lattice: due to the smaller vertical electron beam size in the straight sections, the scraping effect on the small aperture insertion device vacuum vessels, which was creating bremsstrahlung radiation on the beamline, has been eliminated.

The larger distance from the beam edges to the vacuum vessel walls reduces the interaction between the beam and its image current circulating in the vacuum vessel.

In addition, the reduction of vertical beta is a prerequisite for the installation of 10 mm high vacuum vessels (8 mm inner aperture) which will allow the minimum gap to be reduced from the present 16 mm down to 11 mm. As a consequence it will be possible to reduce the undulator period from 42 mm down to 35 mm, thereby providing 50 % more photons for the same X-ray energy. The corresponding brilliances from one undulator segment are shown in Figure 1.

Nevertheless, such a change has a small drawback: the vertical divergence of the photon beam is larger and this could have led to some reduction of photon flux on a few beamlines. To be sure that this was acceptable for their experiments, on 6 October 1996 a few of the concerned beamlines were delivered beam in the low βz lattice. The negative aspects of this new lattice were found to be negligible and, in some cases, beneficial effects were unexpectedly observed. Consequently, the low βz lattice was first implemented for the last run of 1996, beginning on 16 November.

2/3 FILLING MODE

The name of this mode speaks for itself, and the recent switching to this mode at the end of September, in preference over the 1/3 filling, was easily justified by an increase in lifetime from 40 to 50 hours at 200 mA. This rather significant improvement can be explained by the fact that, in this mode, the current per bunch is smaller, thus reducing the Touschek effect, which constitutes one of the lifetime limiting factors with the small 1% coupling.

Running the machine at 200 mA in 2/3 filling mode requires a specific tuning of the RF system to prevent the Higher Order Mode (HOM) related coupled bunch instabilities. These were overcome by carefully adjusting the working temperature of the radio frequence cavities.

HYBRID 4 MODE

The original hybrid mode consisted of a 135 mA 1/3 fill plus one cleaned 7 mA single bunch, whilst hybrid 2 offered a 130 mA 1/3 fill plus two 7 mA single bunches.

The hybrid 4 mode (Figure 2) has been diligently tested during Machine Dedicated Time and will be delivered to the users in the last run of 1996. This version of the hybrid mode provides the answer to delivering 200 mA to the users whilst continuing to offer all the versatility of single bunch (four 5 mA bunches) and 1/3 fill (180 mA).

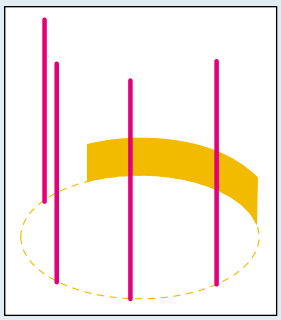

Fig. 2: hybrid 4 mode.

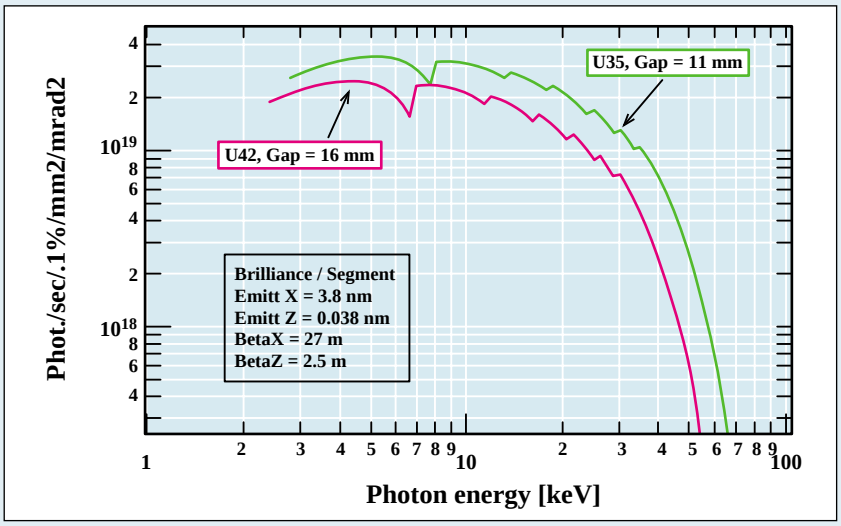

Fig. 1: Brilliances from one undulator segment.

HIGH QUALITY POWER SUPPLY

J.F. BOUTEILLE

ESRF, MACHINE DIVISION

Since summer '95, the ESRF machine can rely on the HQPS (High Quality Power Supply) system to prevent the loss of beam caused by electric storms, which had been previously the main source of interruption to user service during summer time.

This system capable of cleaning the 50 Hz mains is based on 10 units of 1 MVA each, connected in parallel to the 20 kV input line. The stand alone peak power is 7.2 MW with a redundancy of 0.8 MW. Each unit is based on rotating equipment: an alternator, an accumulator and a diesel engine.

Due to the sensitivity of the ESRF machine to mains fluctuations larger than contractual specifications, this cleaning system acts as conditioning equipment which is a key element of the performance of the accelerator complex.

It may be difficult to conceive that the HQPS has the capacity to replace instantaneously the 20 kV mains without any consequences for the storage ring machine. The mechanical components have a tendency to be slow compared to the speed of light when lightning hits the distribution high-voltage lines. Nevertheless the arrangement of the different power components is such that this system reacts to overcome the consequences of the thunderstorm hits. It should be noted that the ESRF load, i.e. the main machine power supplies, are all composed of thyristor driven rectifiers. The storage ring requires about 5 MW to keep the beam and 2 extra MW are necessary to run the injector during the refills.

Each unit of the HQPS system is equipped with different elements as shown in **Figure 1**:
The principal elements are:

- a circuit breaker
- an inductor filter
- an alternator
- an accumulator
- a diesel engine
- a clutch between the diesel engine and the rotor shaft.

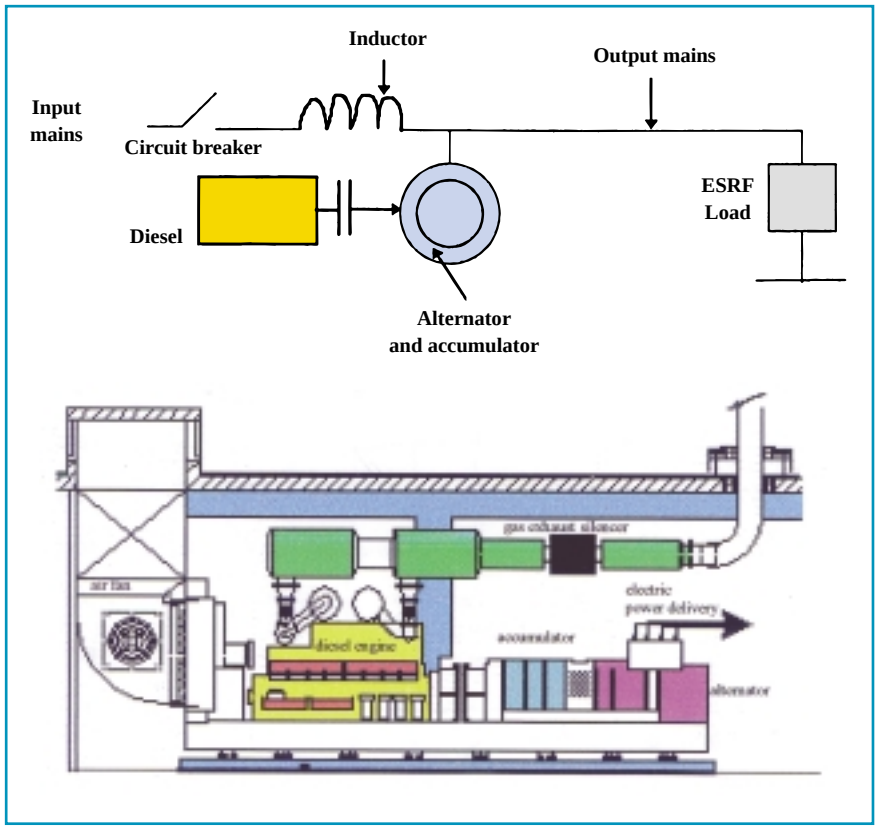

Fig. 1: Main components of the HQPS.

HOW IT WORKS

During normal mode of operation the circuit breaker is closed, the accumulator is charged at 2400 rpm, and the alternator runs at 1500 rpm. In this mode, only the alternator is able to constantly compensate for any drops lower than 20% one phase, or lower than 10%, 3 phases.

When an event occurs on the input mains, the alternator compensates to produce a wave within the +/-5% voltage tolerance. When the drop is such that the energy which needs to be compensated is too great (i.e. greater than a 20% drop lasting more than 100 ms or greater than a 50% drop lasting more than 40 ms), the circuit breaker is opened and the load is fed by the accumulator for a maximum of 5 seconds. In the meantime the diesel engine starts and takes over the load. It takes one second to be at 1500 rpm and then the clutch is closed. The transfer of power between the accumulator and the motor is launched and after two seconds it delivers the nominal power. The diesel engine then starts to recharge the accumulator before reconnecting to the mains, thereby avoiding any vulnerability in the case of a second drop occurring straight after the first one. After the accumulator has recharged and if the mains is within the tolerances for more than one minute, the re-synchronisation procedure on the

external mains starts in order to return to the normal situation. **Figure 2** represents possible observations which could be made in two cases: one with a normal battery start-up (diesel 1 and accumulator 1) and one with a starter fault (diesel 2 and accumulator 2).

The inductor in front of the alternator avoids the consequences of a short-circuit induced by the lightning. It also allows the alternator to keep the output regulated within one percent, during slow input voltage variation of the mains, by varying the reactive power.

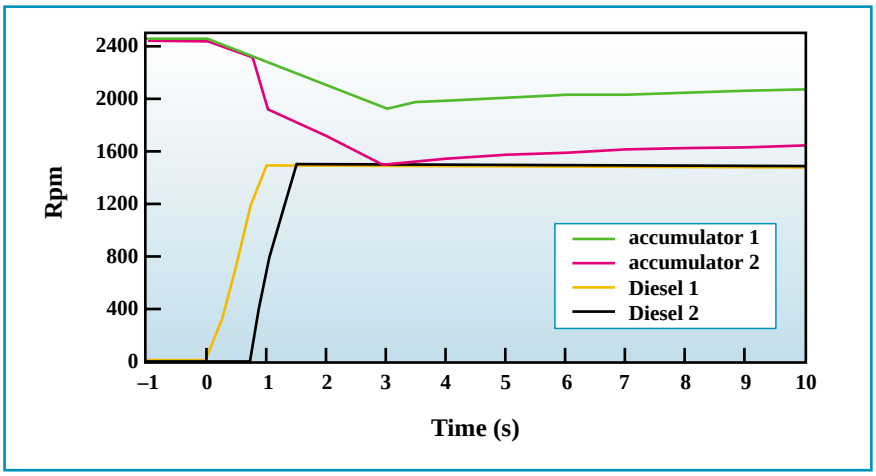

Fig. 2: Two examples of startup of the HQPS, one as a normal battery startup (diesel 1 and accumulator 1) and one with a startup fault (diesel 2 and accumulator 2).

MOTIVATION FOR THE IMPLANTATION OF A POWER PLANT

The quality of the mains was carefully analysed before the installation of HQPS and the following observations have been made:

Over the period mid '92 - mid '93 the following events occurred:

- 135 events out of 198 occurred with less than one hour between them.
- 34 events out of the above 198 were drops greater than 20%
- 14 events out of the above 34 were not only greater than 20% but occurred with less than one hour between them. In such circumstances a normal battery-based system would have failed.

The above figures show that the first initial HQPS scheme (i.e. without diesel engines) would have resulted in a complete machine shutdown 14 times in one year, with several hours needed for recover each time. With the diesel engine option, the diesel engines would have started 34 times a year to protect the machine awaiting a possible multiple repetitive lightning hit.

It should be noted that the 106 cases, corresponding to drops between 10% and 20% which are deep enough to kill the beam, would have been covered by HQPS without the diesels starting.

THE FIRST YEAR OF OPERATION

The HQPS system was made operational in June 1995.

Unlike neighbouring institutes such as SGS Thomson, CNRS, etc., who, every time they are warned of a storm by the system "Meteorage", start up their diesel engine, the ESRF (from June 1995) has not suffered from stormy periods. Over the last 12 months more than 220 drops were recorded on the input, and all of them were nicely smoothed over by the HQPS, thereby preventing beam losses. The diesel engines only started 20 times during that period.

It can definitively be said that this power plant is an added value to the quality of the availability of the beam. The HQPS also contributed significantly to the increase in the Mean Time Between Failure statistic which is now over 40 hours compared to 13 hours two years ago.

For maintenance, the system is permanently watched by a controller who automatically calls the Belgian manufacturer by modem in case of a malfunction. Any minor repairs are dealt with during the bimonthly visits included in the maintenance contract.

In addition to improving the quality of the mains, the system offered the ESRF the possibility to sign an «EJP contract» with the electricity supplier. This contract specifies that electricity is less expensive on «normal days» and much more expensive on «EJP days» (22 days in one year, chosen by the electricity supplier, usually during winter time). This EJP contract has enabled the ESRF to make substantial savings. The global fuel consumption was 538 000 litres for the production of 1854 MWh of clean 20kV mains. The production during storm protection of 186 MWh was added to this. Since then an upgrade in the master controller has led to an improved adaptation of the system to the ESRF's needs. Afterwards the machine was fed with an unperturbed supply. In preparation of the next winter season, a power efficiency modification has been implemented in the driving software. An increase in efficiency of more than 4% is expected during beam delivery and more than 30% during shutdown period.

TROUBLE SHOOTING

On 8 June 1996 a severe storm affected the telephone system, the fire alarm detection system and other, less crucial, elements. Several direct lightning hits were the cause of beam loss, passing through the battery-fed UPS's, protecting the interlock systems.

On 21 August 1996 the beam was lost despite the fact that the HQPS was protecting the machine components. The double direct hit on the ESRF site did not affect the incoming mains but the electromagnetic interference of the lightning on the earth provoked a trip of the radio-frequency system. These two events demonstrate that some perturbations are still capable of directly affecting the machine equipment. At the time of the beam loss, no mains disturbance was recorded.

CONCLUSION

It can now be said that the HQPS system has reached "maturity" and the major software bugs have been eliminated. The added value is well proven and, coupled with the electricity bill savings, it has provided the ESRF with an efficient protection system against mains fluctuations. ■

ESRF Grenoble

17-21 NOVEMBER 1997

SYNCHROTRON RADIATION 50 years

INTERNATIONAL CONFERENCE

HIGHLIGHTS IN X-RAY SYNCHROTRON RADIATION RESEARCH

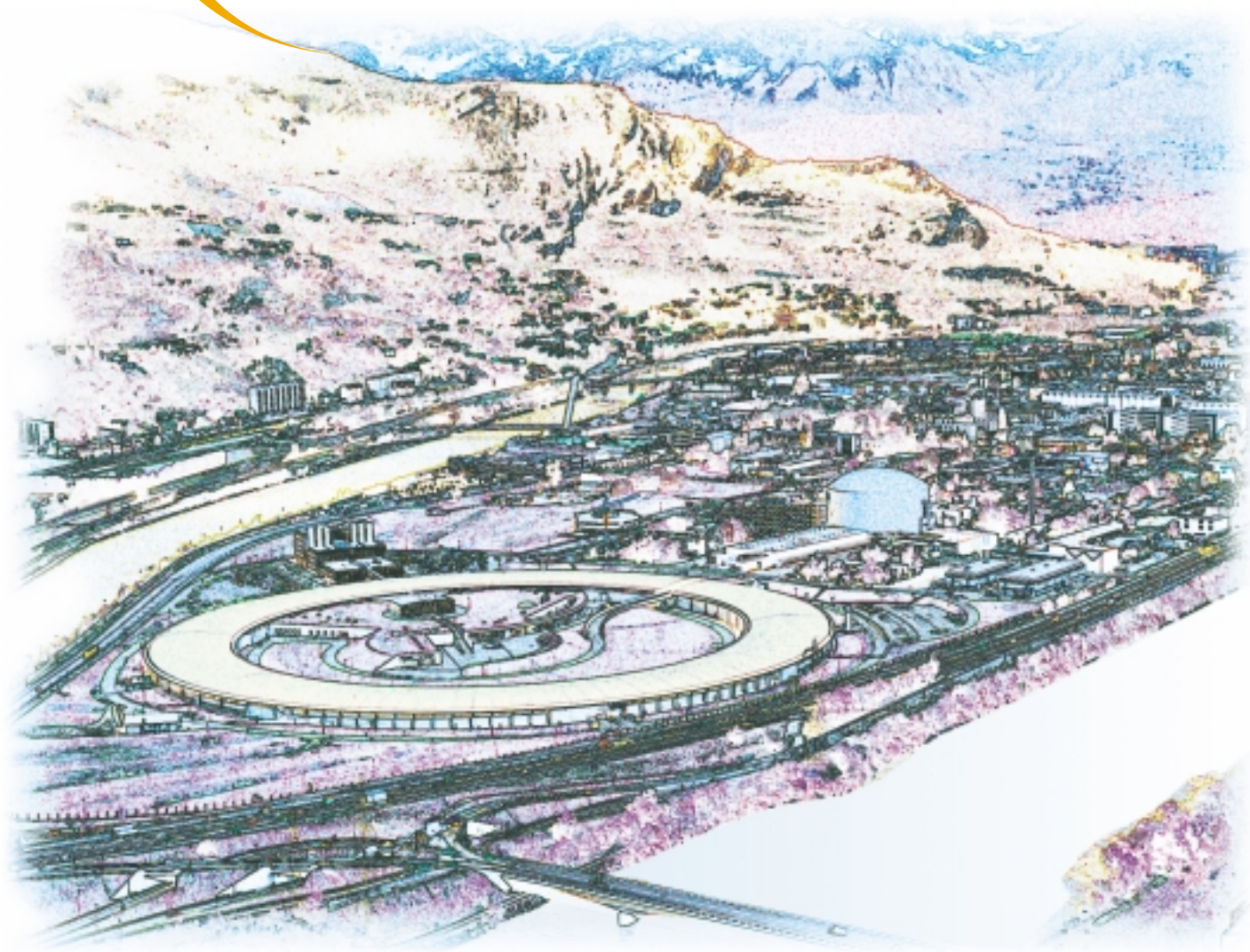

SCIENTIFIC PROGRAMME

- Magnetism
- High pressure
- Soft condensed matter
- Imaging
- Topography
- Biology.

CONTACT

Conference Secretariat
ESRF, BP 220
F38043 Grenoble cedex
Tel. (33) 4 76 88 26 80
Fax (33) 4 76 88 21 60
e-mail: SR50@esrf.fr

The ESRF Newsletter is published by the European Synchrotron Radiation Facility
BP 220, F38043 Grenoble cedex
Editor: Dominique CORNUÉJOLS Tél (33) 4 76 88 20 25

Dépôt légal : 1er trimestre 1997. Printed in France by Saga. Layout by Pixel Project.